

PCCP

Accepted Manuscript



This is an *Accepted Manuscript*, which has been through the Royal Society of Chemistry peer review process and has been accepted for publication.

Accepted Manuscripts are published online shortly after acceptance, before technical editing, formatting and proof reading. Using this free service, authors can make their results available to the community, in citable form, before we publish the edited article. We will replace this *Accepted Manuscript* with the edited and formatted *Advance Article* as soon as it is available.

You can find more information about *Accepted Manuscripts* in the [Information for Authors](#).

Please note that technical editing may introduce minor changes to the text and/or graphics, which may alter content. The journal's standard [Terms & Conditions](#) and the [Ethical guidelines](#) still apply. In no event shall the Royal Society of Chemistry be held responsible for any errors or omissions in this *Accepted Manuscript* or any consequences arising from the use of any information it contains.

Cite this: DOI: 10.1039/c0xx00000x

www.rsc.org/xxxxxx

ARTICLE TYPE

Designing versatile heterogeneous catalysts based on Ag and Au nanoparticles decorated on chitosan functionalized graphene oxide

Rajendiran Rajesh,^a E. Sujanthi,^a S. Senthil Kumar^{b*} and Rengarajan Venkatesan^{a*}*Received (in XXX, XXX) Xth XXXXXXXXX 20XX, Accepted Xth XXXXXXXXX 20XX*

DOI: 10.1039/b000000x

Herein we report the covalent grafting of chitosan on graphene oxide (GO) followed by a simple approach for anchoring silver (AgNPs) and gold (AuNPs) nanoparticles on to the chitosan grafted graphene oxide surface by NaBH₄ reduction method. The catalytic activity of the prepared heterogeneous GO grafted chitosan stabilized silver and gold nanocatalysts (GO-Chit-Ag/AuNPs) has been explored for the reduction of aromatic nitroarenes and degradation of hazardous azo dyes in presence of NaBH₄. Both the catalysts were found to exhibit excellent catalytic activity towards the reduction of aromatic nitroarenes and azo dyes degradation. Furthermore, the nanocatalysts were found to be selective towards the reduction of nitro groups in the halonitroarenes without any dehalogenation under mild conditions.

1. Introduction

Owing to the exceptional electronic, physical and mechanical properties, graphene sheets that consist of single sheet of sp² carbon remain as a class of the most widespread research materials.^{1,2} Graphene oxide (GO), an important derivative of graphene has rapidly become a promising material among the researchers as it has a large surface area and also it can be easily prepared by the chemical oxidation of graphite.³ GO possesses various reactive functional groups including hydroxyl, epoxy, and carboxylic acid and these groups provide an artery for functionalization of GO for desired applications.^{4,8} Interestingly, functionalized GO continues to exist as an excellent support for anchoring the catalysts since these materials can bridge with the substrate molecules through non-covalent bonding interactions that include hydrogen bonding, hydrophobic, π - π * stacking and electrostatic interactions, which respond to stimulate the activating groups of the substrates near the catalyst.^{9,10} Moreover, GO sheets supported with the catalysts are highly efficient because the catalysts contained on both the sides of the sheet will be accessible for the substrate molecules.

Catalysis by silver and gold nanoparticles (Ag and Au NPs) incorporated on solid matrix has drawn immense interest in recent years.¹¹⁻¹⁴ The Ag/AuNPs tend to aggregate easily due to their highly active surface atoms and subsequently leading to reduced catalytic activity. Considering the advantages of GO as a catalytic support into account, researchers have attempted to immobilize these metal NPs on GO. Recently the reduction of nitroarenes has been reported on a catalytic system based on AuNPs/reduced graphene oxide hybrid.¹⁵ However, the amount of oxygen functionalities present to stabilize the nanoparticles were less and therefore only a minimum of AuNPs could be incorporated. This shortcoming could be overcome by grafting polymers on GO and consequently increasing the sites for

encapsulation of metal NPs on GO. Our focus here is to graft chitosan (Chit), a biocompatible, biodegradable and non-toxic natural polymer on GO and the chitosan polymer with more number of -NH₂, -OH functional groups may facilitate stabilization of more number of Ag/AuNPs. There were few reports in the recent past on the improved mechanical properties of GO/Chit hybrid system.¹⁶⁻¹⁸ To the best of our knowledge, there is no report on the catalytic activity of Ag/AuNPs stabilized on chitosan functionalized GO (GO-Chit-Ag/AuNPs).

Aromatic amines are conceded to be the potent intermediates in the bulk production of many analgesics and antipyretic drugs, dyeing agents, agricultural chemicals, surfactants and polymers. The conventional route for the preparation of these aromatic amines is based on the reduction of corresponding nitro derivatives using catalytic hydrogenation and other chemical reduction methods.^{19,20} In chemical reduction method numerous reducing agents have been utilized for the reduction of nitroarenes, with the most classic being Fe-HCl in stoichiometric quantities. This method requires iron in large quantities, however the yield is very poor and a huge amount of Fe-FeO sludge is generated which poses severe effluent problem and thus the entire reaction setup becomes environmentally hazardous.²¹⁻²³ Significant research contributions have been made in the chemoselective reduction of aromatic nitrocompounds with H₂ using heterogeneous catalysts based on gold nanoparticles supported on TiO₂ or Fe₂O₃, nanoscale cobalt oxide supported on a carbon-nitrogen surface and iron oxide particles surrounded by a nitrogen-doped carbon layer.²⁴ Hence, there is a continuous need for an effective and environmentally benign approach for the selective reduction of aromatic nitro compounds. Reduction using NaBH₄ as the hydride source can be considered as an alternative route, but the reduction cannot be achieved in the absence of any catalyst.²⁴⁻²⁸ Therefore, development of a catalytic system for selective and efficient reduction of aromatic

nitroarenes is highly desired.

The textile manufacturing process which involves preparation and utility of various dyes partly introduce these dyestuffs into aquatic systems leading to environmental pollution and health hazards.²⁹⁻³³ Azo dyes have been extensively used in textiles, leather and paper industries and constitute ca. 50% of all dyes produced and thus, efficient degradation of azo dyes has become a challenging task for the environmental chemists.³⁴ Many different methodologies are being adopted to treat the dye effluents that include adsorption tactics,³⁵ biological degradations,³⁶ Fenton-like reactions,³⁷ and photocatalysis.³⁸ The adsorption methodology resulted in the transfer of pollutants from waste water to solid wastes and the traditionally employed biological degradation delivered poor efficiency. In case of Fenton-like reactions, the subsequent treatment of ferrous slurry and also the requirement of H_2O_2 lead to complexity. Thorough degradation of azo dyes is said to be achieved using photocatalysis, whereas the most employed photocatalytic material, TiO_2 is active only in the ultraviolet range because of its wide band gap. Immense efforts have been made towards the modification of TiO_2 with an objective of developing visible light-active photocatalysts, whereas their practical applications

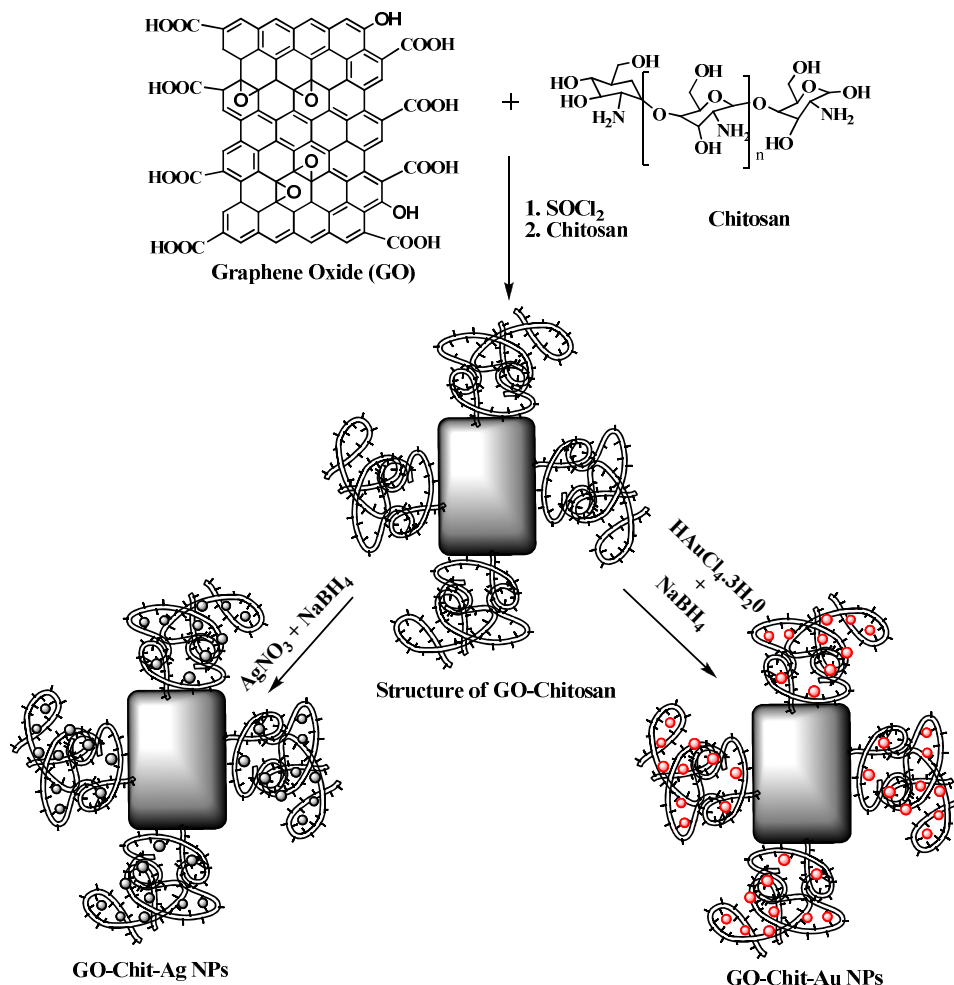
are limited since the quantum yield is yet not satisfactory.^{39,40} Thus, the development of a simple method/material for the efficient degradation of azo dyes has gained enormous significance.

In the present investigation, we have developed an efficient heterogeneous catalytic system to meet both these important tasks. We have covalently grafted chitosan with GO, followed by the stabilization of Ag and AuNPs on the chitosan grafted GO (GO-Chit) to yield GO-Chit-Ag/AuNPs nanocatalysts. The covalent grafting of Chit on GO and the stabilization of metal nanoparticles have been thoroughly characterized. The catalytic activities of the prepared GO-Chit-Ag/AuNPs towards the reduction of aromatic nitroarenes and degradation of azo dyes have been evaluated. To further verify the selectivity of GO-Chit-Ag/AuNPs nanocatalysts, selective reduction of nitro groups in halonitroarenes has also been demonstrated.

2. Experimental

2.1 Chemicals

Graphite, fine powder of particle size $50\ \mu m$ was obtained from Sigma Aldrich USA. Tetrachloroauric (III) acid trihydrate, silver



Scheme 1 Schematic illustration of Ag/AuNPs decorated GO-Chit.

nitrate, chitosan (~90% deacetylation), sulfuric acid, potassium permanganate, hydrogen peroxide, sodium nitrate, thionyl chloride, sodium borohydride, methyl orange and congo red were purchased from Merck, India. All the chemicals were used without further purification. Double distilled water was used throughout the experiment.

2.2 Measurements

The covalent grafting of chitosan polymer on the GO was confirmed by FT-IR spectroscopy (Nicolet 6700 FT-IR spectrometer using KBr method). The interaction between GO and Chit was characterized using Raman spectroscopy (Witec Confocal Raman instrument (CRM200) with Ar ion laser 514.5 nm). The crystallinity of the GO, GO-Chit and GO-Chit stabilized Ag/AuNPs was studied using powder XRD analysis (XpertPRO Pananalytical X-ray diffractometer employing Cu K α radiation). Surface morphology and elemental composition of the catalyst were investigated using HITACHI S-3400N Scanning Electron Microscope (SEM) along with Energy dispersive-X-ray (EDX) spectroscopy (Thermo SuperDry II attached with SEM). Size and morphology of the dispersed Ag/AuNPs on GO-Chit were obtained from Tecnai F-30 High Resolution Transmission Electron Microscope (HR-TEM). Further insight into grafting of the chitosan was obtained from thermal gravimetric analyzer (TG-DTA-Q 600 SDT) from room temperature to 800 °C. The reduction of *p*-nitrophenol to *p*-aminophenol and degradation of azo dyes were monitored by Optical absorption spectrum Ocean optics (HR4000) spectrophotometer.

2.3 Preparation of chitosan functionalized graphene oxide decorated with Ag/Au nanoparticles (GO-Chit-Ag/AuNPs)

GO was prepared from graphite based on Hummers and Offeman's method with slight modifications and the typical procedure has been presented in our previous report.⁵ In brief, the prepared GO (0.5 g) was suspended in SOCl₂ (30 mL) and stirred for 24 h at 70 °C. This solution was filtered, washed with anhydrous tetrahydrofuran (THF) and then dried under vacuum for 24 h at room temperature, generating graphene oxide with acyl chloride side chain (GO-COCl) (0.4953 g).

GO-COCl (0.5 g) was first homogenized with 20 mL water in an ultrasonic bath for 60 min. The GO-COCl suspension was transferred to a solution containing chitosan in 2% acetic acid (1 g in 20 mL) and the mixture was stirred for 1 h, followed by sonication for 20 min to make the solution nearly homogeneous and then the stirring was continued for another 24 h at room temperature. The obtained chitosan grafted GO (GO-Chit) solution was filtered and washed with double distilled water until the pH reached 7 and dried at 65 °C under vacuum.

Ag/AuNPs were stabilized on the chitosan grafted GO (GO-Chit) based on the following procedure: GO-Chit (50 mg) was dispersed in 10 mL of de-ionized water by sonication for 30 min. To this dispersion, 10 mL of 0.01 M AgNO₃ solution was added drop wise and the mixture was stirred for 1 h. 10 mL of 0.01 M NaBH₄ was added to the above mixture and the stirring was continued for another 24 h. The product was filtered, washed thrice with double distilled water and then dried overnight under vacuum to yield GO-Chit decorated with AgNPs (GO-Chit-AgNPs, 43 mg). GO-Chit decorated with AuNPs (GO-Chit-AuNPs) was prepared using similar procedure as that of the

AgNPs with slight modifications. Tetrachloroauric (III) acid trihydrate was used instead of silver nitrate and a higher concentration of 0.05 M NaBH₄ was used for the reduction of gold salt and the procedure resulted in 40 mg of GO-Chit-AuNPs. The developed Ag and AuNPs (GO-Chit-Ag/AuNPs) obtained were insoluble in water or any other organic solvents. They can be well dispersed in water and solvents such as ethanol and methanol upon sonication under higher frequency, whereas they are moderately dispersible in dimethyl formamide and dimethyl sulphoxide.

2.4 Method for reduction of *p*-nitrophenol using GO-Chit-Ag/AuNPs

The catalytic activity of prepared nanomaterials Ag/Au NPs-GO-Chit) towards the reduction of nitroarenes in presence of aqueous NaBH₄ was studied by the model experiment carried out using UV-Vis spectrophotometer using 0.01 mM (3 mL) aqueous solution of 4-nitrophenol, 0.1 mM (50 μ L) NaBH₄ and 5 mg of Ag/AuNPs in a 3 mL UV cuvette. The reaction was monitored at 400 nm at different time intervals.^{19,20}

2.5 Procedure for selective reduction of nitro groups of various halo nitroarenes using (GO-Chit-Ag/AuNPs), in presence of NaBH₄

In a typical reaction, 50 mg of catalyst (GO-Chit-Ag/AuNPs) and 1 mM of halonitro compound were added to 50 mL of water. Then 10 mM of NaBH₄ was added slowly to the reaction mixture and the mixture was stirred at room temperature. The reaction was monitored through TLC and reaction mixture was quenched by extracting the organic derivatives with ethyl acetate. The organic solvent was evaporated under vacuum to give the product of corresponding amine compound. Then the reduced amine products were confirmed by melting point, IR and ¹H NMR. The conversion yield was monitored through GC.²⁵

2.6 Method for degradation of organic azo dyes in aqueous solution by GO-Chit-Ag/AuNPs

The catalytic degradation of organic azo dyes namely methyl orange (MO) and congo red (CR) have been examined using UV-Vis spectroscopy. 3 mL of 10⁻⁵ M aqueous solutions of MO and CR were taken in a quartz cuvette and 5 mg of GO-Chit-Ag/AuNPs heterogeneous nano catalysts were added to the aqueous dye solutions separately. To the reaction mixture 50 μ L of 0.1 M NaBH₄ was added and the decreasing absorption maximum of the azo dyes were recorded.

3. Results and discussion

3.1 Covalent grafting of chitosan polymer on graphene oxide

The covalent link between chitosan and GO was clearly elucidated by FT-IR spectroscopy. Fig. 1a shows the spectra of pure graphite with bands at 1651 and 1380 cm⁻¹ corresponding to the stretching vibrations of C=C and C-C groups respectively. In the case of GO (Fig. 1b), three new broad and intense peaks were found to appear at 3435, 1734, and 1259 cm⁻¹ which may be due to the characteristic stretching vibration of O-H, C=O and C-O groups respectively. In the FT-IR spectrum of acylated graphene oxide (GO-COCl) shown in Fig. 1c, the peak at 3435 cm⁻¹ disappears completely along with a shift of C=O peak to 1694

cm⁻¹ and with the introduction of a new peak at 694 cm⁻¹, all of which indicate the formation of C-Cl bond.⁴¹⁻⁴³ The covalent immobilisation of chitosan on to the GO was confirmed in Fig. 1d through the appearance of aliphatic (-CH₂) and amide (-CONH) peaks at 2095 and 1645 cm⁻¹ respectively and also the peak appearing at 3480 cm⁻¹ is attributed to the stretching vibration of free -NH and O-H groups of grafted chitosan polymer.¹⁶ Thus, the FT-IR results clearly demonstrate the covalent grafting of chitosan polymer on GO.

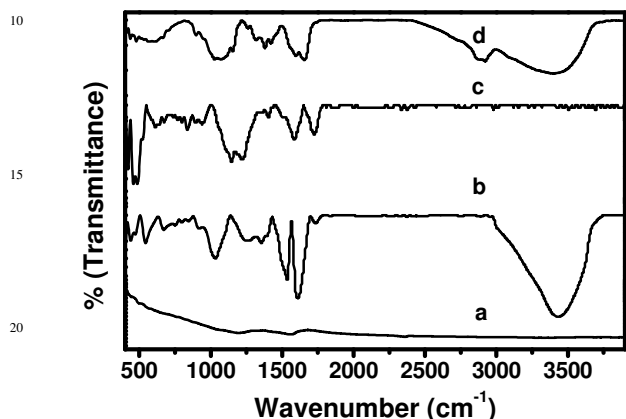


Fig. 1 FT-IR spectra of (a) pure graphite, (b) GO, (c) GO-COCl and (d) GO-Chit.

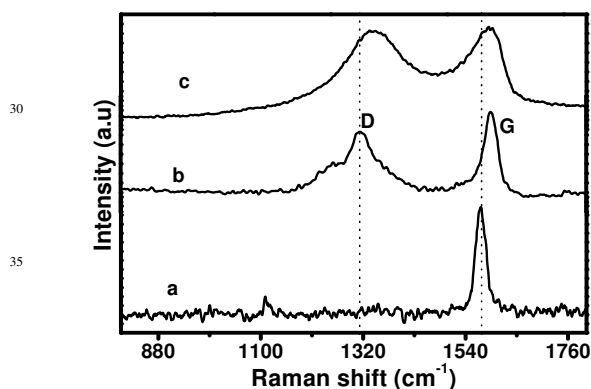


Fig. 2 Raman spectra of (a) pure graphite, (b) GO and (c) GO-Chit.

Further investigation on chitosan grafting and the properties of GO layers were studied by Raman spectroscopy. Fig. 2 (a, b, c) depicts the Raman spectra of pure graphite, GO and GO-Chit respectively. All the samples exhibited two major bands between 1330 and 1590 cm⁻¹ corresponding to the D and G bands respectively.^{44,45} The D and G band arises from the activation of first order scattering process of k-point phonons of the A_{1g} (Csp³) atom, whereas the G band arises due to the E_{2g} phonons of the (Csp²) atom. Generally, the D band is relatively weak or nearly invisible in perfect graphite lattice and we observed the same in our case (Fig. 2a). The spectrum of GO shows broad and intense D band appearing at 1315 cm⁻¹ and this could be due to the increasing number of oxygen containing functional groups and the increasing sp³ carbon atom as a result of oxidation.^{46,47} Also, the G band of the GO shifts about 24 cm⁻¹ (1574 to 1598 cm⁻¹) due to the disengagement of graphene oxide layers and increasing

oxygen functionalities (Fig. 2b). In the case of GO-Chit (Fig. 2c), the enhanced intensity in D band can be attributed to the glucopyranose ring of chitosan. The D/G ratios are found to be 0.204, 0.77 and 0.9786 for pure graphite, GO and GO-Chit respectively. The highest D/G ratio of GO-Chit substantiates the successful functionalization of the chitosan polymer on GO.

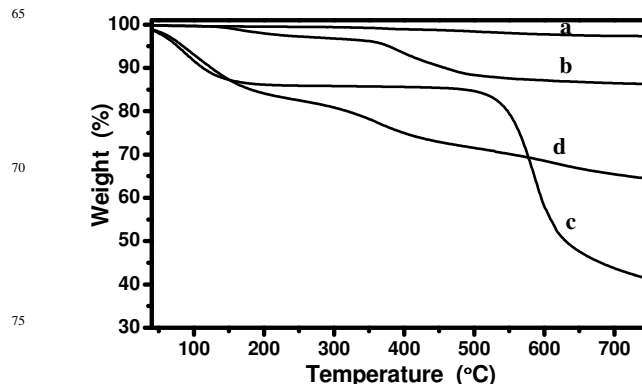


Fig. 3 TGA analysis of (a) pure graphite, (b) GO, (c) chitosan and (d) GO-Chit.

The grafted content of the chitosan polymer with GO can be calculated from the weight loss between 200 and 800 °C. TGA results shown in Fig. 3a demonstrate no appreciable weight loss for pure graphite. In the case of GO (Fig. 3b), considerable weight loss of about ~13% occurs between 120-300 °C due to the pyrolysis of labile oxygen functional groups of -OH, -COOH and epoxy groups.^{48,49} As can be seen in Fig. 3c, pure chitosan exhibits about 11% weight loss in the temperature range of 30-100 °C due to evaporation of the absorbed water and 47% of weight loss between 450-700 °C due to the degradation of polysaccharide units. The thermogram of GO-Chit in Fig. 3d exhibits gradual weight loss of about 16% below 400 °C which is likely due to the loss of glucopyranose ring of chitosan and the residual functional groups of GO sheets. Interestingly, the total weight loss of the grafted chitosan has decreased (~36%) after functionalization with GO and this reveals that most of the epoxide and hydroxyl groups of GO were successfully functionalized by covalent interaction with chitosan.

3.2 Decoration of Ag/AuNPs on chitosan functionalized GO

The X-ray diffraction studies were carried out in order to compare the crystalline nature of GO, GO-Chit and Ag/AuNPs (stabilized on GO-Chit). The powder XRD spectrum of pure graphite (Fig. 4a) shows a strong intense diffraction peak at 26.52° (002) which represents an interlayer distance of 0.34 nm, corresponding to the hexagonal lattice of graphite. From Fig. 4b, it can be observed that the multilayer graphite peak (26.52°) has completely vanished and new diffraction peak appears at 12.5° implying the formation of single layer of graphene oxide.⁵⁰ In the case of GO-Chit (Fig. 4c), diffraction peaks appearing at 2θ = 20.1°, 47.6°, 54.3° and 77.6° indicate the semicrystalline nature of grafted chitosan polymer.^{51,52} The XRD pattern depicted in Fig. 4d and 4e reveal the formation of GO-Chit-AgNPs and GO-Chit-AuNPs, with the average size (calculated from Scherrer's equation, $D = K\lambda/\beta_s \cos\theta$)⁵³ of 20 nm and 5 nm respectively. It can be observed that AuNPs exhibits high crystallinity compared to that of AgNPs and the complete disappearance of peak at 20.1° in Fig. 4e may be due to the high crystalline nature of AuNPs.

Diffraction patterns suggest that both GO-Chit-Ag/AuNPs exist in face centered cubic (fcc) form. Diffraction patterns of AgNPs at $2\theta = 38.2^\circ, 44.3^\circ, 64.6^\circ$ and 77.4° correspond to (111), (200), (220), and (311) lattice planes respectively and that of AuNPs at $2\theta = 38.3^\circ, 44.7^\circ, 64.6^\circ$ and 77.8° correspond to (111), (200), (220), and (311) lattice planes respectively.⁵⁴⁻⁵⁶

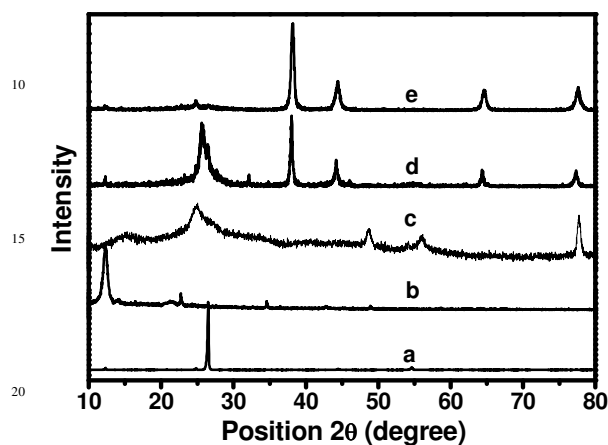


Fig. 4 Powder X-ray diffraction patterns of (a) pure graphite, (b) GO, (c) GO-Chit, (d) GO-Chit-AgNPs and (e) GO-Chit-AuNPs.

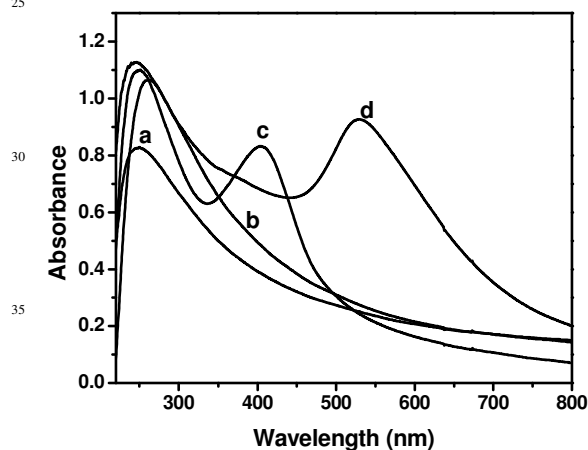


Fig. 5 UV-Vis spectra of (a) GO, (b) GO-Chit, (c) GO-Chit-AgNPs and (d) GO-Chit-AuNPs.

The successful synthesis of Ag/AuNPs decorated over GO-Chit was confirmed further using UV-Vis spectroscopy. In Fig. 5a, the UV-Vis spectrum of GO exhibits absorption maximum at 250 nm indicating the formation of different oxygen functionalities in GO. In the case of GO-Chit (Fig. 5b), the absorption peak undergoes a red shift to 260 nm and this may be due to the overlapping of $\pi-\pi^*$ transition of the graphene backbone and $n-\pi^*$ transition of the chitosan polymer. This result manifests the successful grafting of chitosan polymer on GO. In Fig. 5c and 5d, the appearance of surface plasmon resonance peaks at 410 nm and 530 nm, once again confirm that the silver and gold nanoparticles are stabilized successfully on the GO-Chit to yield GO-Chit-Ag/AuNPs.^{49,57}

The surface morphology of the GO-Chit and the Ag/AuNPs decorated on GO-Chit (GO-Chit-Ag/AuNPs) were monitored

using scanning electron microscope (SEM). In Fig. 6a, the SEM image of pure graphite shows flake like structure indicating the multi-layered morphology. In contrast, Fig. 6b shows a highly transparent thin layer for the oxidised form of graphene (GO) and this may be due to the formation of single layer of GO. In the case of GO-Chit (Fig. 6c), the SEM image displays a randomly mixed rope like structure and this could be attributed to the formation of blend of chitosan polymer with GO. The decoration of Ag/AuNPs on GO-Chit can be observed in Fig. S1d and S1e (see ESI). The images represent homogeneous dispersion of Ag and AuNPs on GO-Chit. Additionally, the details of elemental analysis (EDX) are presented along with SEM images in Fig. S1 (see ESI).

The dispersion and the size of the synthesized Ag/AuNPs were investigated using HR-TEM. In Fig. 7a and 7b, the TEM images demonstrate the homogeneous deposition of AgNPs on the GO-Chit without agglomeration. Fig. 7c illustrates the high magnification TEM image of AgNPs and it can be observed that the size of the dispersed nanoparticles is about ~ 20 nm. The complete dispersion of anchored AuNPs is observed in Fig. 7d which indicates that there is no agglomeration of nanoparticles. Fig. 7e demonstrates TEM image of AuNPs with high magnification and can be seen that the size of the prepared nanoparticles is about ~ 5 nm. The selected area diffraction (SAED) image of GO-Chit-AuNPs is presented in Fig. 7f, which shows the bright diffraction rings from inner to outer, and can be indexed as (111), (200), (220), (311) and (222) planes respectively confirming the highly crystalline nature of AuNPs.⁵⁰ We further analysed Ag and Au NPs size distributions from the HR-TEM images of the GO-Chit-Ag/Au NPs. A size distribution analysis of the AgNPs reveals an average size of 20 nm, ranging from 5 to 40 nm (Fig. S3b). However, in the case of AuNPs stabilized in GO-Chit, the average size of the AuNPs is 5 nm, ranging from 2 to 14 nm (Fig. S3d).

The BET surface area of pure graphite, GO, GO-Chit-Ag/AuNPs were measured by nitrogen adsorption measurements and depicted in Table S1 ESI. The synthesized GO exhibits significantly increased surface area ($185 \text{ m}^2/\text{g}$) than that of pure graphite ($8.7 \text{ m}^2/\text{g}$).⁴³ Interestingly, the BET surface area of the Ag and Au NPs stabilized on GO grafted chitosan has increased to $290 \text{ m}^2/\text{g}$ and 293 respectively. The grafted content of the chitosan induces the stabilization of more number of Ag and AuNPs, which is the origin for substantial increase in BET adsorption values.

3.3 Catalytic reduction of nitroarenes using GO-Chit-Ag/AuNPs

The catalytic activity of the prepared GO-Chit-Ag/AuNPs were tested towards the reduction of *p*-nitrophenol to *p*-aminophenol in presence of NaBH_4 . The model reduction kinetic experiment was studied using 0.01 mM aqueous solution of *p*-nitrophenol and 0.1 mM NaBH_4 in presence of 5 mg catalyst in a 3 mL UV cuvette³² and the conversion was monitored using the absorbance recorded at 400 nm (Fig. 8). The pseudo first order rate constant was estimated to be $5.5 \times 10^{-3} \text{ s}^{-1}$ and $3.8 \times 10^{-3} \text{ s}^{-1}$ for GO-Chit-AgNPs and GO-Chit-AuNPs respectively (Table 1). No reaction was observed in the presence of pure graphite or with graphene oxide or with bare GO-Chit. The excellent catalytic activity obtained in presence of GO-Chit-Ag/AuNPs is mainly attributed

to the Ag and AuNPs firmly and uniformly stabilized in the highly blended network of the chitosan polymer.

Furthermore, the efficacy of GO-Chit-Ag/AuNPs towards the selective reduction of aromatic nitro groups in presence of other reducing functionalities was investigated. Few attempts have been made towards the selective reduction of nitroarenes in the recent past, using copper NPs,⁵⁸ palladium NPs⁵⁹ catalysts and also using Pt nanoparticles containing membrane as a catalyst.⁶⁰ However, all the above discussed selective aromatic nitro reduction methods were associated with few drawbacks including low yield and also the requirement of high temperature $\sim 120^\circ\text{C}$ and high pressures for the entire process making the reduction process highly tedious.

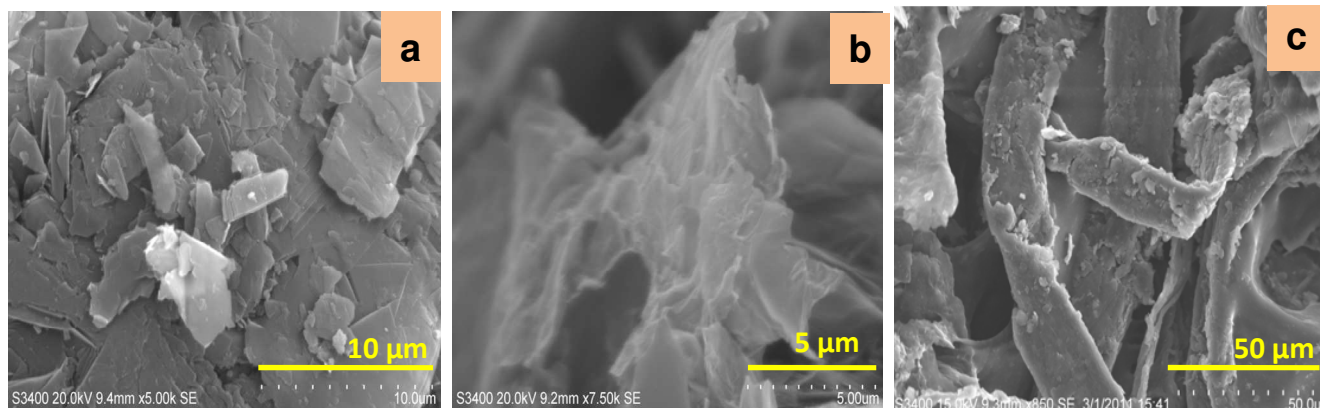
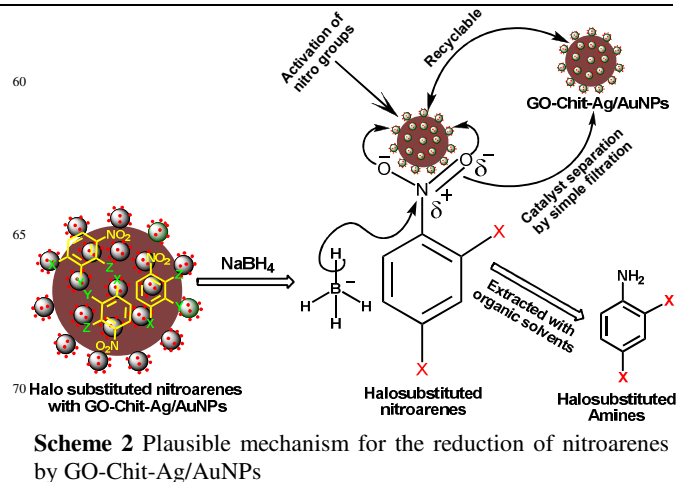


Fig. 6 SEM images of (a) pure graphite, (b) GO and (c) GO-Chit.

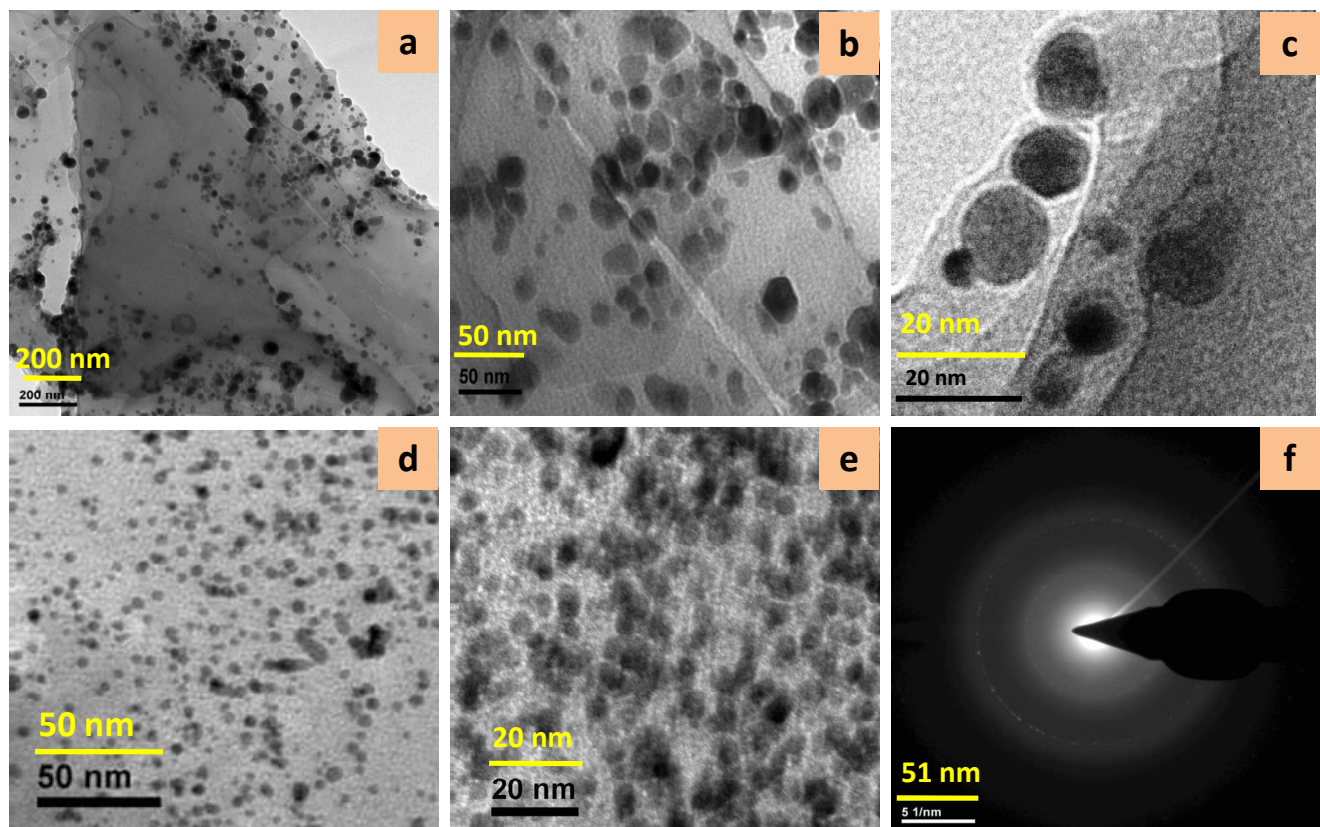


Fig. 7 HR-TEM images of (a, b, c) GO-Chit-AgNPs and (d, e, f) GO-Chit-AuNPs respectively.

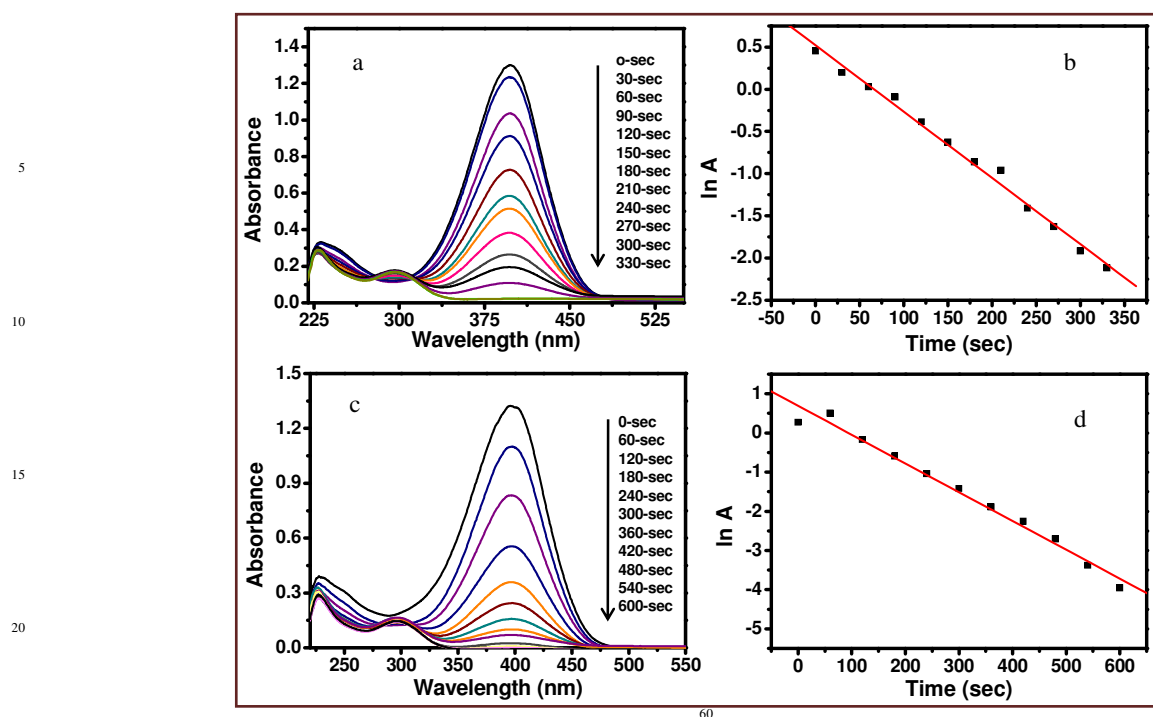


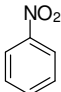
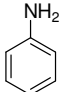
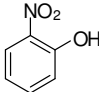
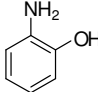
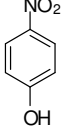
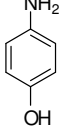
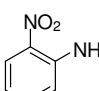
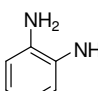
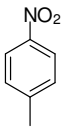
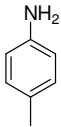
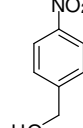
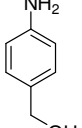
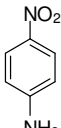
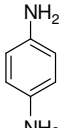
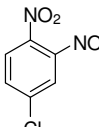
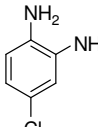
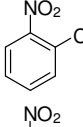
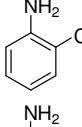
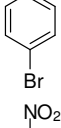
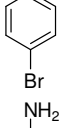
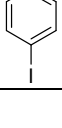
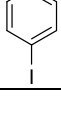
Fig. 8. (a) UV-Vis spectra for the reduction of *p*-nitrophenol measured in different time intervals using (a) GO-Chit-AgNPs, (c) GO-Chit-AuNPs, Fig. 8(b, d) demonstrate $\ln A$ vs Time plot for the reduction of *p*-nitrophenol using Ag/AuNPs decorated GO-Chit respectively.

Table 1 Systematic literature survey for the reduction of *p*-nitrophenol and corresponding rate constant at room temperature.

Entry	Sample	Carrier system	Metal	Rate constant (k) for the reduction of <i>p</i> -nitrophenol ^j	Ref.
1	GO-Chit-Ag/AuNPs ^a	Chitosan	Ag	$5.5 \times 10^{-3} \text{ s}^{-1}$	This work
			Au	$3.8 \times 10^{-3} \text{ s}^{-1}$	This work
2	AuNPs/Resin ^b	Ion-exchange resin	Au	$0.16 \times 10^{-3} \text{ s}^{-1}$	19
3	AgNPs/PS-PEGMA ^c	Polymer brush	Ag	$0.33 \times 10^{-3} \text{ s}^{-1}$	20
4	NiNPs/Mesoporous Silica ^d	Silica	Ni	$2.8 \times 10^{-3} \text{ s}^{-1}$	21
5	AuNPs/MgO ^e	MgO	Au	$4.4 \times 10^{-3} \text{ s}^{-1}$	22
6	Pt/Au/Pd NPs/ Silica ^f	Silica	Pt	$0.0014 \times 10^{-3} \text{ s}^{-1}$	23
			Au	$0.71 \times 10^{-3} \text{ s}^{-1}$	
			Pd	$0.715 \times 10^{-3} \text{ s}^{-1}$	
7	AuNPs/Fe ₃ O ₄ ^g	Fe ₃ O ₄	Au	$0.72 \times 10^{-3} \text{ min}^{-1}$	24
8	AuNPs/PEO-b-PAA ^h	PEO-b-PAA	Au	$0.333 \times 10^{-3} \text{ min}^{-1}$	25
9	AuNPs/Breynia rhamnoides ⁱ	Breynia rhamnoides	Au	$4.6 \times 10^{-3} \text{ s}^{-1}$	26

^aReactions were catalyzed by GO grafted chitosan stabilized Ag and Au NPs. ^b Ion exchange resin supported AuNPs. ^c Polystyrene-Polyethylene glycol supported AgNPs. ^d Mesoporous Silica supported NiNPs. ^e Magnesium oxide supported AuNPs. ^f Porous silica supported Pt/Au and Pd NPs. ^g Iron oxide supported AuNPs. ^h Poly(ethylene oxide)-block-poly(acrylic acid) supported AuNPs. ⁱ Breynia rhamnoides in AuNPs. ^j Apparent rate constants obtained under optimized conditions. NaBH₄ was used as the reducing agent in all the cases.

Table 2 Catalytic reduction of various nitro aromatics over Ag/AuNPs-GO-Chitosan^{a, b}

Entry	Substrate	Product	GO-Chit-AgNPs (Time, min)	GO-Chit-AuNPs (Time, min)	Yield ^c (%)
1			40	100	100
2			45	110	100
3			45	110	100
4			45	110	100
5			40	100	100
6			40	100	100
7			45	110	100
8			80	200	66
9			45	120	100
10			45	120	100
11			45	120	100

10

^aReaction conditions: 50 mg of catalyst, 1 mmol of substrate, 10 mmol of NaBH₄, 50 mL of water, stirring at room temperature.^bReused catalyst after separation from the reaction mixture.^cConversion yield was monitored through GC.

Hence, in the present study we used the prepared catalysts to reduce different nitro substituted aromatics under mild conditions. The efficacy of the prepared catalyst (GO-Chit-Ag/AuNPs) in reducing various nitro derivatives is presented in Table 2 and the plausible mechanism for the reduction of nitroarenes in presence of GO-Chit-Ag/AuNPs is shown in Scheme 2. The fascinating character of our catalyst is the quantitative selective reduction of halo-substituted nitrobenzenes without any dehalogenation (Table 2, entries 8-11). All the tested mononitroarene derivatives have resulted in 100% conversion to corresponding amine compounds, whereas the dinitroarene derivative (Table 2, entry 8) has resulted in only 60-66% conversion. The remaining 35-40% might have resulted in the formation of monoamine derivative which can be reduced further to diamine derivative through an additional reduction step.

3.4 Degradation of organic azo dyes using Ag/AuNPs/GO-Chit as heterogeneous nanocatalysts

Since the developed nanocatalysts have shown excellent catalytic activity for the reduction of nitroarenes, we extended our interest in examining the performance of GO-Chit-Ag/AuNPs towards another challenging task, i.e., towards the degradation of different hazardous organic dye molecules. Methyl orange (MO) and Congo red (CR) which are used as commercial colorants for dyeing in textile industries were chosen as the representative substrates for evaluating the catalytic activity of our nanocatalysts. The degradation reaction was performed at room temperature in the presence of NaBH₄ as a reducing agent and the reaction was monitored with the help of UV-Visible spectrometer. MO and CR dyes were found to exhibit absorption maxima in the visible region of light at 465 and 495 nm respectively and hence the catalytic degradation of these dyes was monitored by observing the change in absorbance of these peaks and then the pseudo-first order rate constants were calculated.

In order to optimize the suitable condition for effective degradation, experiments were carried out with different concentrations of NaBH₄ and various amounts of Ag/AuNPs. Maximum degradation was found to be achieved in the presence of 50 μL of 0.1 M NaBH₄ and 5 mg of GO-Chit-Ag/AuNPs and hence the same concentration of NaBH₄ and the nanoparticles were maintained for further investigations on the degradation activity of Ag/AuNPs. The absorbance remains constant in presence and absence of light, AgNPs and simple NaBH₄ for many days, suggesting that MO and CR dyes by themselves are stable. Degradation of these dyes was not found to proceed in the absence of either NaBH₄ or the Ag/AuNPs. Fig. 9a and 9b show the UV-Vis kinetic spectra for the degradation of MO and CR by GO-Chit-AgNPs in presence of NaBH₄ at different time intervals. This shows that when these dyes are mixed with GO-Chit-AgNPs in presence of NaBH₄, the absorbance start to decrease and it reaches to immeasurably low value (near to zero) and the solution become colourless. Further exposure lead to no change in the absorbance in the whole spectrum, which indicates the complete degradation of the dyes. Fig. 9c and 9d show ln A vs Time plots for the degradation of MO and CR by GO-Chit-AgNPs in presence of NaBH₄ and the apparent pseudo-first order rate constants were calculated to be 4.41 × 10⁻³ sec⁻¹ and 3.4 × 10⁻³ sec⁻¹. The degradation rate constants calculated for both the

prepared nanocatalysts towards degradation of MO and CR were found to be comparable with or better than the reported values (Table 3).

The investigations discussed in section 3.3 and 3.4 reveals that the decoration of Ag and AuNPs into the chitosan functionalized GO results in promising catalytic activities. The interesting catalytic activity observed with GO-Chit-Ag/AuNPs towards the reduction of nitroarenes and the degradation of azo dyes is attributed to the following reasons (a) high surface area of the GO grafted chitosan which helps to adsorb more number of organic substrates, (b) large number of -NH₂ and -OH functional groups present in the chitosan polymer could assist in uniform stabilization of Ag/AuNPs leading to high catalytic active surface, (c) hydrophilic nature of the chitosan polymer and hydrophobic nature of the graphene which could attract the substrate towards the catalytic sites for easy reaction, (d) activation of aromatic -NO₂ groups through binding of oxygen atoms of nitrobenzene with the dispersed Ag/AuNPs (for reduction of nitroarenes) and (e) activation of azo nitrogen of dyes through binding of sulphur, nitrogen and oxygen atoms with Ag/AuNPs and thus weakening the azo double bond via conjugation (for degradation of dyes). All these features either together or separately lead to the facile reduction of nitroarenes and efficient dye degradation. GO-Chit-AgNPs were found to exhibit higher catalytic activity for both the reactions compared to that of GO-Chit-AuNPs and it may be due to the greater oxygen affinity of Ag which stabilizes the substrate molecules in the catalytic site.

3.5 Influence of catalytic dosage towards the reduction of *p*-nitrophenol and azo dye degradations

In order to examine the effect of amount of catalyst on the rate of reduction of *p*-nitrophenol, the reaction was carried out in varying amount of GO-Chit-Ag/AuNPs by 1 mg increment, in presence of identical concentration of NaBH₄ and *p*-nitrophenol. It can be observed from Fig. S4, that the rate of reduction of *p*-nitrophenol increases with the amount of catalyst added upto 5 mg, and further increase in the amount of catalyst did not contribute for any significant enhancement in the reduction rate. Hence, 5 mg of the nanocatalysts has been chosen as the optimum dosage for efficient catalytic reduction of *p*-nitrophenol. Similar results were obtained for degradation of MO and CR azo dyes (Fig. S5-S26).

3.6 Recyclability

Stability and recyclability are important for the practical applications of catalysts. Hence, the recyclability of the prepared GO-Chit-Ag/AuNPs were tested towards the reduction of *p*-nitrophenol. After the reduction of *p*-nitrophenol, both the catalysts could be easily recovered by centrifugation and washing three times with distilled water. The reusability of the GO-Chit-Ag/AuNPs was studied after the first cycle and then the catalysts were recycled for 10 successive cycles without significant loss of its activity (Fig. S27). Similarly the recyclability experiments were examined for degradation of MO and CR azo dyes. These results indicate that the developed catalytic materials exhibited excellent stability and recyclability.

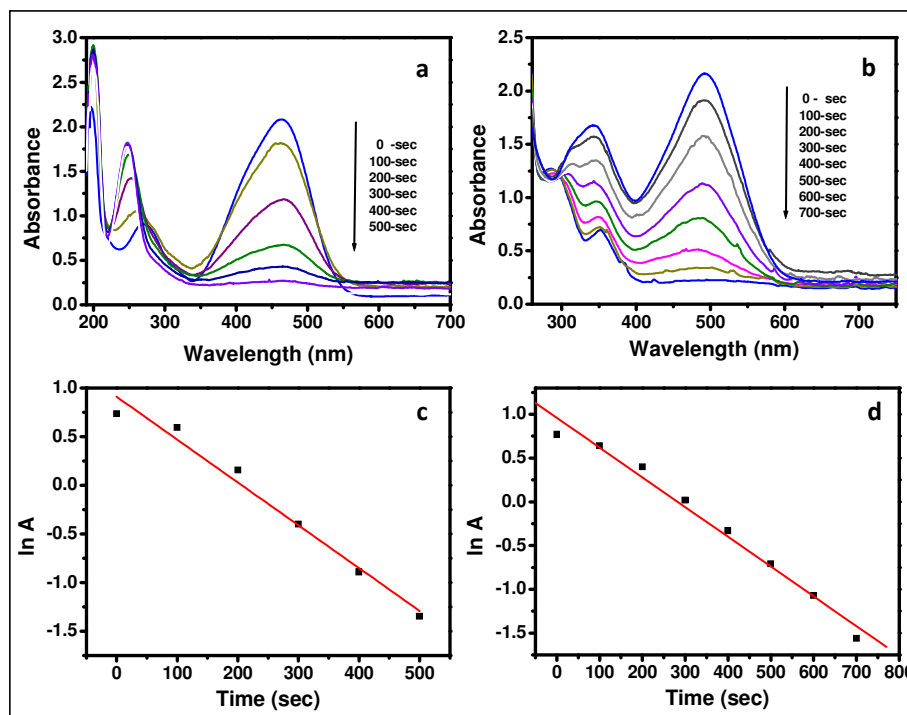
5
10
15
20

Fig. 9 UV-Vis kinetic spectra for the degradation of (a) methyl orange and (b) congo red by AgNPs-GO-Chit. In A vs Time plot for the degradation of (c) methyl orange and (d) congo red by AgNPs-GO-Chit.

Table 3 Systematic literature survey for the degradation of methyl orange and congo red azo dyes and corresponding rate constant at room temperature.

25
30
35

Entry	Samples	Carrier system	Metals	Rate constants (k) for the degradation of		Ref.
				Methyl orange	Congo red ^k	
1	Ag/GO-Chit ^a	Chitosan/GO	Ag	$4.41 \times 10^{-3} \text{ s}^{-1}$	$3.4 \times 10^{-3} \text{ s}^{-1}$	This work
	Au/GO-Chit ^b	Chitosan/GO	Au	$3.01 \times 10^{-3} \text{ s}^{-1}$	$2.14 \times 10^{-3} \text{ s}^{-1}$	This work
2	Ag/Au/Pt/ Tannic acid ^c	Tannic acid	Ag	$583 \times 10^{-3} \text{ min}^{-1}$	-	61
			Au	$4.9 \times 10^{-3} \text{ min}^{-1}$	-	75
			Pt	$2.9 \times 10^{-3} \text{ min}^{-1}$	-	
3	P25TiO ₂ /GO ^d	P25	Ti	$116 \times 10^{-3} \text{ min}^{-1}$	-	62
4	TiO ₂ /PW ₁₂ ^e	PAH	W	$46.5 \times 10^{-3} \text{ min}^{-1}$	-	63
5	TiO ₂ /CNTs ^f	CNTs	Ti	$37.3 \times 10^{-3} \text{ min}^{-1}$	-	64
6	Alumina/CuO ^g	Alumina	Cu	-	$567 \times 10^{-3} \text{ min}^{-1}$	65
7	Thioacetamide/NiS ^h	Thioacetamide	Ni	-	$72 \times 10^{-3} \text{ min}^{-1}$	66
8	TiO ₂ ⁱ	TiO ₂ (TNA)	Ti	-	$12.5 \times 10^{-3} \text{ min}^{-1}$	67
9	P25TiO ₂ /SiO ₂ ^j	SiO ₂	Ti	-	$0.003 \times 10^{-3} \text{ min}^{-1}$	68

^{a, b}Reactions were catalyzed by GO grafted chitosan polymer stabilized Ag and Au NPs. ^cTannic acid supported Ag/Au/Pt NPs. ^dGraphene oxide supported P25TiO₂NPs. ^eTitanium oxide supported tungsten phosphate nanoparticles. ^fCarbon nanotube supported TiO₂NPs. ^gAlumina supported Copper oxide nanoparticles. ^hNickel sulphate nanoparticles. ⁱTitanium oxide nanotube arrays NPs. ^jP25Titanium oxide NPS supported Silicone oxide nanoparticles. ^kApparent rate constants calculated under optimized reaction conditions. Entries 1, 2 and 6 have utilized NaBH₄ as the reducing agent and entries 3-5 and 7-9 were based on photocatalytic degradation.

45

4. Conclusion

In summary, we have designed an efficient catalytic system upon stabilizing the Ag and AuNPs on to the chitosan functionalized graphene oxide. The prepared heterogeneous Ag/AuNPs have shown excellent catalytic activity towards the reduction of nitroarenes and degradation of toxic azo dyes. In addition, our catalytic system has exhibited adequate selectivity towards the reduction of nitro groups without any dehalogenation in halonitroarenes. The developed catalysts have shown their proficiency through the achieved rates of the reactions and selectivity. Considering the wide potential of graphene oxide as an encapsulating material for a variety of nanoparticles, the approach improved here may channel to new possibilities for the development of various hybrid systems via numerous functionalities for diversified applications.

Acknowledgements

We gratefully acknowledge the University Grants Commission (UGC), Govt. of India, New Delhi, for funding the research project (F. No 39-782/2010 (SR)). The authors also acknowledge the services rendered by Central Instrumentation Facility (CIF), Pondicherry University.

Notes

^a Department of Chemistry, Pondicherry University, Puducherry-605014, India. Corresponding Authors: Dr. R. Venkatesan, Fax: +91-413-2654415; E-Mail: venkatesanr.che@pondiuni.edu.in

^b Environmental & Analytical Chemistry Division, School of Advanced Sciences, VIT University, Vellore-632014, India. E-Mail: senthilanalytical@gmail.com

[†] Electronic Supplementary Information (ESI) available: Detailed SEM, EDX, TEM and Surface analyser of GO, GO-Chit and GO-Chit-Ag/AuNPs. Detailed UV-Vis kinetics for the effective catalytic dosage for reduction of *p*-nitrophenol, degradation of MO and CR azo dyes. See DOI: 10.1039/b000000x/

References

- 1 A. A. Balandin, S. Ghosh, W. Bao, I. Calizo, D. Teweldebrhan, F. Miao, *Nano Lett.*, 2008, **8**(3), 902.
- 2 S. Stankovich, D. A. Dikin, G. H. B. Dommett, K. M. K. Lhaas, E. J. Zimney, E. A. Stach, R. D. Piner, S. T. Nguyen, R. S. Ruoff, *Nature*, 2006, **442**(7100), 282.
- 3 D. A. Dikin, S. Stankovich, E. J. Zimney, R. D. Piner, G. H. B. Dommett, G. Evmenenko, S. T. Nguyen, R. S. Ruoff, *Nature*, 2007, **448**(7152), 457.
- 4 D. Li, R. B. Kaner, *Science*, 2008, **320**(5880), 1170.
- 5 C. Lee, X. Wei, J. W. Kysar, J. Hone, *Science*, 2008, **321**(5887), 385. R. Rajesh, R. Venkatesan, *Journal of Molecular Catalysis A: Chemical*, 2012, **359**, 88.
- 6 J. S. Bunch, A. M. V. Zande, S. S. Verbridge, I. W. Frank, D. M. Tanenbaum, J. M. Parpia, H. G. Craighead, P. L. M. Euen, *Science*, 2007, **315**(5811), 490.
- 7 K. S. Novoselov, A. K. Geim, S. V. Morozov, D. Jiang, Y. Zhang, S. V. Dubonos, I. V. Grigorieva, A. A. Firsov, *Science*, 2004, **306**(5696), 666.
- 8 K. Jayakumar, R. Rajesh, V. Dharuman, and R. Venkatesan, *Methods in Molecular Biology*. 2013, **201**, 1039. T. Kuila, A. Kumar Mishra, P. Khanra, N. H. Kim and J. H. Lee, *Nanoscale*, 2013, **5**, 52.
- 9 B. F. Machado and P. Serp, *Catal. Sci. Technol.*, 2012, **2**, 54.
- 10 M. J. M. Allister, J. L. Li, D. H. Adamson, H. C. Schniepp, A. A. Abdala, J. Liu, M. Herrera-Alonso, D. L. Milius, R. Car, R. K. Prud'homme and I. A. Aksay, *Chem. Mater.*, 2007, **19**, 4396.
- 11 D. Astruc, F. Lu, and J. R. Aranzas, *Angew. Chem. Int. Ed.*, 2005, **44**, 7852. S. Schimp, M. Lucas, C. Mohr, U. Rodemerck, A. Bruckner, J. Radnik, H. Hofmeister, P. Claus, *Catalysis Today*, 2002 **2592**, 1.
- 12 Y. Li, X. Fan, J. Qi, J. Ji, S. Wang, G. Zhang, F. Zhang, *Materials Research Bulletin*, 2010, **45**, 1413.
- 13 J. Zheng, Y. Dong, W. Wang, Y. Ma, J. Hu, X. Chen and X. Chen, *Nanoscale*, 2013, **5**, 4894.
- 14 G. M. Scheuermann, L. Rumi, P. Steurer, W. Bannwarth and R. Mulhaupt, *J. Am. Chem. Soc.*, 2009, **131**, 8262..
- 15 Y. Choi, H. S. Bae, E. Seo, S. Jang, K. H. Park and B. S. Kim, *J. Mater. Chem.*, 2011, **21**, 15431.
- 16 X. Yang, Y. Tu, L. Li, S. Shang, X. M. Tao, *Applied Materials & Interfaces*, 2010, **2**, 1707. S. Stankovich, D. A. Dikin, R. D. Piner, K. A. Kohlhaas, A. Kleinhammes, Y. Jia, Y. Wu, S. T. Nguyen, R. S. Ruoff, *Carbon*, 2007, **45**, 1558.
- 17 H. C. Schniepp, J. L. Li, M. J. M. Allister, H. Sai, M. H. Alonso, D. H. Adamson, R. K. Prudhomme, R. Car, D. A. Saville, I. A. Aksay, *J. Phys. Chem. B*, 2006, **110**, 8535. Y. Pan, H. Bao, and L. Li, *Appl. Mater. Interfaces*, 2011, **3**, 4819.
- 18 Y. C. Si, E. T. Samulski, *Nano Lett.*, 2008, **8**, 1679. Y. Guo, X. Sun, Y. Liu, W. Wang, H. Qiu, J. Gao, *Carbon*, 2012, **50**, 2513. S. F. Wang, L. Shen, W. D. Zhang, Y. J. Tong, *Biomacromolecules*, 2005, **6**, 3067.
- 19 A. Agarwal, and P. G. Tratnyek, *Environ. Sci. Technol.*, 1996, **30**, 153. S. Panigrahi, S. Basu, S. Praharaaj, S. Pande, S. Jana, A. Pal, S.K. Ghosh, *J. Phys Chem. C*, 2007, **111**, 4596.
- 20 K. Stella, F. C. Lynch, M. Xiaomei, L. W. Jin, A. Jane, H. H. Carol, C. A. Gabriella, F. L. Beane, A. Jennifer, R. L. Hou, P. D. Sandler, C. R. M. Alavanja, *Int. J. Cancer*, 2009, **124**, 1206. Y. Lu, Y. Mei, R. Walker, M. Ballauff, M. Drechsler, *Polymer*, 2006, 4985.
- 21 O. A. de, P. E. Kagohara, H. Leandro, A. V. Joao, C. H. S. Iracema, R. Crusius, C. R. Claudete, Paula, L. M. A. Porto, *Enzyme Microb. Technol.*, 2007, **42**, 65. S. Z. S. Gai, F. He, Y. Dai, P. Gao, L. Li, Y. Chen, and P. Yang, *Nanoscale*, 2014, **6**, 7025.
- 22 U. Sharma, N. Kumar, P. K. Verma, V. Kumar and B. Singh, *Green Chem.*, 2012, **14**, 2289. K. Layek, M. L. Kantam, M. Shirai, D. N. Hamane, T. Sasakid and H. Maheswaran, *Green Chem.*, 2012, **14**, 3164. R. Dey, N. Mukherjee, S. Ahammed and B. C. Ranu, *Chem. Commun.*, 2012, **48**, 7982.
- 23 M. Baron, E. Metay, M. Lemairea and F. Popowycz, *Green Chem.*, 2013, **15**, 1006. L. Zhou, C. Gao and W. Xu, *Langmuir.*, 2010, **26**(13), 11217.
- 24 A. Corma and P. Serna, *Science*, 2006, **313**, 332. F. A. Westerhaus, R. V. Jagadeesh, G. Wienhofer, M.-M. Pohl, J. Radnik, A.-E. Surkus, J. Rabeah, K. Junge, H. Junge, M. Nielsen, A. Bruckner and M. Beller, *Nat. Chem.*, 2013, **5**, 537. R. V. Jagadeesh, A.-E. Surkus, H. Junge, M.-M. Pohl, J. Radnik, J. Rabeah, H. Huan, V. Schünemann, A. Brückner and M. Beller, *Science*, 2011, **342**, 1073.
- 25 M. Tumma, R. Srivastava, *Catal. Commun.*, 2013, **37**, 64. F. Lin and R. Doong, *J. Phys. Chem. C*, 2011, **115**, 6591. M. David, D. S. Bhattacharjee, Y. Wen, L. M. Bruening, *Langmuir*, 2009, **25**, 1865.
- 26 E. Seo, J. Kim, Y. Hong, Y. S. Kim, D. Lee and B. S. Kim, *J. Phys. Chem. C*, 2013, **117**, 11686. M. Shokouhimehr, J. E. Lee, S.I. Han, T. Hyeon, *Chem. Commun.*, 2013, **49**, 4779. K. Kuroda, T. Ishida, M. Haruta, *J. Mol. Catal. A: Chem.*, 2009, **9**, 298.
- 27 C. Lee, X. Wei, J. W. Kysar, J. Hone, *Science*, 2008, 321(5887), 385. A. Gangula, R. Podila, M. Ramakrishna, L. Karanam, C. Janardhana, and A. M. Rao, *Langmuir*, 2011, **27**, 15268.
- 28 M. L. Crossley, *Ind. Eng. Chem.*, 1922, **14**, 802.
- 29 Y. Mei, G. Sharma, Y. Lu, M. Ballauff, *Langmuir*, 2005, **21**, 12229.
- 30 P. G. Rieger, H. M. Meir, M. Gerle, U. Vogt, T. Groth, H. J. Knackmuss, *J. Biotechnol.*, 2002, **94**, 101.
- 31 G. M. Liu, X. Z. Li, J. C. Zhao, *Environ. Sci. Technol.*, 2000, **34**, 3982.
- 32 M. H. Habibi, A. Hassanzadeh, S. Mahdavi, *J. Photochem. Photobiol. A*, 2005, **172**, 89.

- 32 C. Hu, X. X. Hu, L. S. Wang, J. H. Qu, A. M. Wang, *Environ. Sci. Technol.*, 2006, **40**, 7903.
- 33 M. Janus, A. W. Morawski, *Appl. Catal. B*, 2007, **75**, 118.
- 34 H. Zhang, D. Chen, L. V. Xiaojun, Y. Wang, H. Chang, Jinghong Li, *Environ. Sci. Technol.*, 2010, **44**, 1107.
- 35 J. Pengfei, J. Zhang, F. Chen, M. Anpo, *Appl. Catal. B*, 2009, **85**, 148.
- 36 F. J. Cervantes, A. G. Espinosa, M. A. M. Reynosa, J. R. R. Mendez, *Environ. Sci. Technol.*, 2010, **44**, 1747.
- 10 37 J. Fernandez, J. Bandara, A. Lopez, P. Buffat, J. Kiwi, *Langmuir*, 1999, **15**, 185..
- 38 J. Lee, H. S. Shim, M. Lee, J. K. Song, D. Lee, *J. Phys. Chem. Lett.*, 2011, **2**, 2840.
- 39 C. Amaresh, Pradhan, K. M. Parida, B. Nanda, *Dalton Trans*, 2011, **40**, 7348..
- 15 40 J. Zhang, Z. Xiong, X. S. Zhao, *J. Mater. Chem.*, 2011, **21**, 3634.
- 41 K. Jayakumar, R. Rajesh, V. Dharuman, R. Venkatesan, J. H. Hahn, S. Karutha Pandian, *Biosensors and Bioelectronics*, 2012, **31**, 406.
- 42 X. Kang, J. Wang, H. Wu, I. A. Aksay, J. Liu, Y. Lin, *Biosensors and Bioelectronics*, 2009, **25**, 901.
- 20 43 R. Feng, G. Guan, W. Zhou, C. Li, D. Zhang and Y. Xiao, *J. Mater. Chem.*, 2011, **21**, 3931.
- 44 Y. P. Sun, K. Fu, Y. Lin, W. Huang, *Acc. Chem. Res.*, 2002, **35**, 1096.
- 25 45 C. Cioffi, S. Campidelli, C. Sooambar, M. Marcaccio, G. Marcolongo, M. Meneghetti, D. Paolucci, F. Paolucci, C. Ehli, G. M. A. Rahman, V. Sgobba, D. M. Guldi, M. Prato, *J. Am. Chem. Soc.*, 2007, **129**, 3938.
- 46 N. Konstantin, Kudin, B. Ozbas, C. Hannes, Schniepp, K. Robert, Prudhomme, A. Ilhan, Aksay, R. Car, *Nano Lett.*, 2008, **8**, 36.
- 30 47 S. Sarkar, E. Bekyarova, S. Niyogi, C. R. Haddon, *J. Am. Chem. Soc.*, 2011, **133**, 3324.
- 48 S. Wakelanda, R. Martineza, K. J. Greyb, C. C. Luhrs, *Carbon*, 2010, **48**, 3463.
- 35 49 S. Z. Zu, B. H. Han, *J. Phys. Chem. C*, 2009, **113**, 13651.
- 50 R. Rajesh, S. Sendhil Kumar, R. Venkatesan, *New J. Chem.*, 2014, **38**, 1551.
- 51 V. K. Rana, M. C. Choi, J. Y. Kong, G. Y. Kim, M. J. Kim, S. H. Kim, S. Mishra, R. P. Singh, C. S. Ha, *Macromol. Mater. Eng.*, 2011, **296**, 131.
- 40 52 Y. Zhao, X. Song, Q. Song and Z. Yin. *Cryst. Eng. Comm.*, 2012, **14**, 6710.
- 53 D. Philip, C. Unnib, S. A. Aromala, V. K. Vidhua, *Spectrochimica Acta Part A*, 2011, **78**, 899.
- 45 54 F. Bei, X. Hou, S. L. Y. Chang, G. P. Simon, and D. Li, *Chem, Eur. J*, 2011, **17**, 5958.
- 55 S. S. Shankar, A. Ahmad, M. Sastry, *Biotechnol. Prog*, 2003, **19**, 1627.
- 56 J. Huang, Q. Li, D. Sun, Y. Lu, Y. Su, X. Yang, H. Wang, W. Shao, N. He, J. Hong, C. Chen, *Nanotechnology*, 2007, **18**, 105.
- 50 57 H. Wang, X. Qiao, J. Chen, S. Ding, *Colloids Surf. A.*, 2005, **256**, 111.
- 58 T. Subramanian and K. Pitchumani, *Chem Cat Chem.*, 2012, **4(12)**, 1917.
- 55 59 J. M. Campelo, D. Luna, R. Luque, J. M. Marinas and A. A. Romero, *Chem Sus Chem.*, 2009, **2**, 18.
- 60 R. Nie, J. Wang, L. Wang, Y. Qin, P. Chen, Z. Hou, *Carbon*, 2012, **50**, 586.
- 61 N. Gupta, H. P. Singh, R. K. Sharma, *Journal of Molecular Catalysis A: Chemical*, 2011, **335**, 248.
- 60 62 S. M. Torres, L. M. P. Martinez, J. L. Figueiredo, J. L. Faria, A. M.T. Silva, *Applied Surface Science*, 2013, **275**, 361.
- 63 P. Niu and J. Hao, *Langmuir*, 2011, **27**, 13590.
- 64 Y. J. Xu, Y. Zhuang and X. Fu, *J. Phys. Chem. C*, 2010, **114**, 2669.
- 65 65 D. Jana and D. Goutam, *RSC Adv.*, 2012, **2**, 9606.
- 66 H. Guo, K. Yingchang, D. Wang, K. Lin, R. Shen, J. Chen, W. Weng, *J Nanopart Res.*, 2013, **15**, 1475.
- 67 T. S. Natarajan, K. Natarajan, H. C. Bajaj and J. R. J. Tayade, *Ind. Eng. Chem. Res.*, 2011, **50**, 7753.
- 70 68 H. R. Jafry, M. V. Liga, Q. Li and A. R. Barron, *Environ. Sci. Technol.*, 2011, **45**, 1563.

Figures and Tables

Designing versatile heterogeneous catalysts based on Ag and Au nanoparticles decorated on chitosan functionalized graphene oxide

Rajendiran Rajesh,^a E. Sujanthi,^a S. Senthil Kumar^{b*} and Rengarajan Venkatesan^{a*}

a Department of Chemistry, Pondicherry University, Puducherry-605014, India.

Corresponding authors: Fax; +91-413-2655987; Tel: +91-413-2654415;

E-mail: venkatesanr.che@pondiuni.edu.in (R. Venkatesan)

b Environmental & Analytical Chemistry Division, School of Advanced Sciences, VIT University, Vellore-632014, India.

E-Mail: senthilanalytical@gmail.com (S. Senthil Kumar)

Figures captions :

1. **Fig. 1** FT-IR spectra of (a) pure graphite, (b) GO, (c) GO-COCl and (d) GO-Chit.
2. **Fig. 2** Raman spectra of (a) pure graphite, (b) GO and (c) GO-Chit.
3. **Fig. 3** TGA analysis of (a) pure graphite, (b) GO, (c) chitosan and (d) GO-Chit.
4. **Fig. 4** Powder X-ray diffraction patterns of (a) pure graphite, (b) GO, (c) GO-Chit, (d) GO-Chit-AgNPs and (e) GO-Chit-AuNPs.
5. **Fig. 5** UV-Vis spectra of (a) GO, (b) GO-Chit, (c) GO-Chit-AgNPs and (d) GO-Chit-AuNPs.
6. **Fig. 6** SEM images of (a) pure graphite, (b) GO and (c) GO-Chit.
7. **Fig. 7** HR-TEM images of (a, b, c) GO-Chit-AgNPs and (d, e, f) GO-Chit-AuNPs respectively.
8. **Fig. 8.** (a) UV-Vis spectra for the reduction of *p*-nitrophenol measured in different time intervals using (a) GO-Chit-AgNPs, (c) GO-Chit-AuNPs, Fig. 8(b, d) demonstrate $\ln A$ vs Time plot for reduction of *p*-nitrophenol Ag/AuNPs decorated GO-Chit respectively.

9. **Fig. 9** UV-Vis kinetic spectra for the degradation of (a) methyl orange and (b) congo red by AgNPs-GO-Chit. In A vs Time plot for the degradation of (c) methyl orange and (d) congo red by AgNPs-GO-Chit.

Scheme 1 Schematic illustration of Ag/AuNPs decorated GO-Chit.

Scheme 2 Plausible mechanism for the reduction of nitroarenes by GO-Chit-Ag/AuNPs

Tables captions

Table 1 Systematic literature survey of the reduction of *p*-nitrophenol and corresponding rate constant at room temperature.

Table 2 Catalytic reduction of various nitro aromatics over Ag/AuNPs-GO-Chitosan.

Table 3 Systematic literature survey of the degradation of methyl orange and congo red azo dyes and corresponding rate constant at room temperature.

Figures:

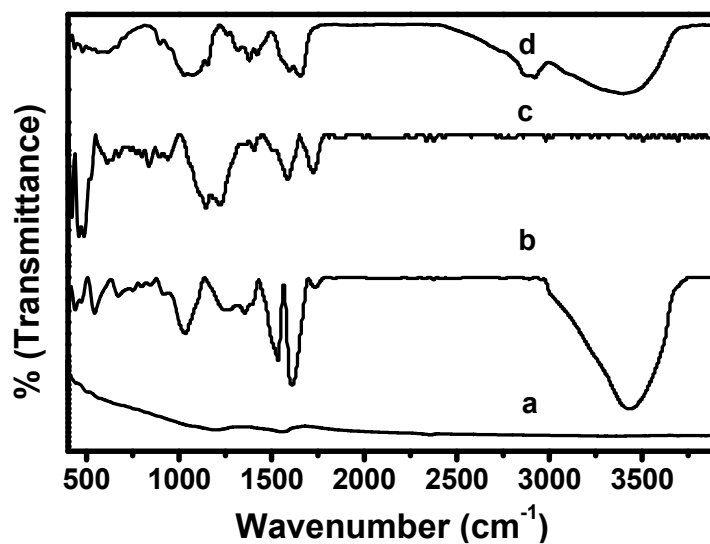


Fig. 1 FT-IR spectra of (a) pure graphite, (b) GO, (c) GO-COCl and (d) GO-Chit.

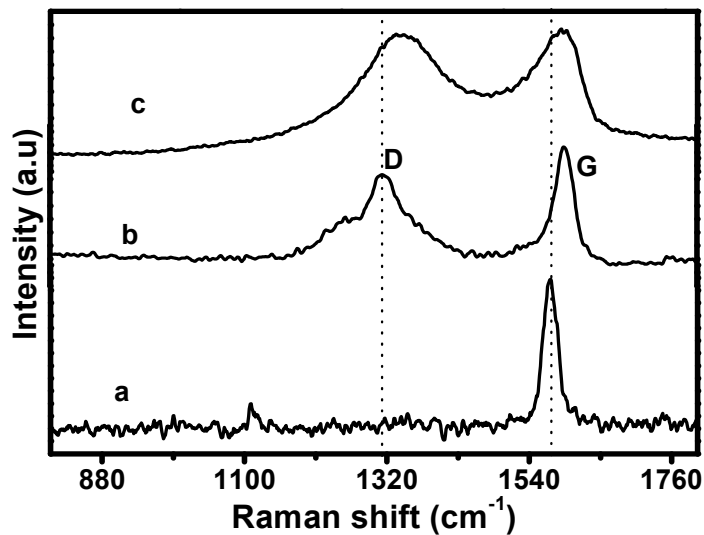


Fig. 2 Raman spectra of (a) pure graphite, (b) GO and (c) GO-Chit.

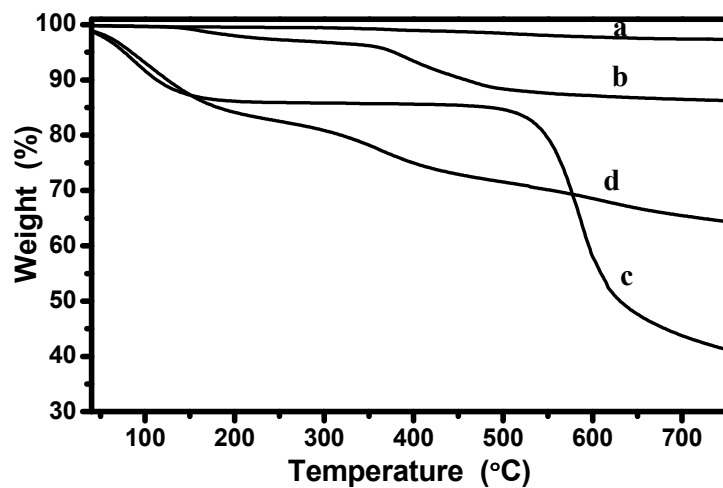


Fig. 3 TGA analysis of (a) pure graphite, (b) GO, (c) chitosan and (d) GO-Chit.

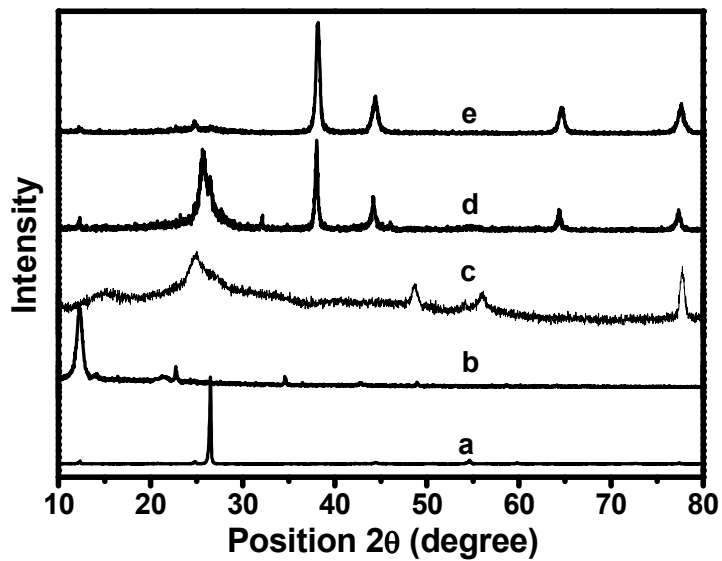


Fig. 4 Powder X-ray diffraction patterns of (a) pure graphite, (b) GO, (c) GO-Chit, (d) GO-Chit-AgNPs and (e) GO-Chit-AuNPs.

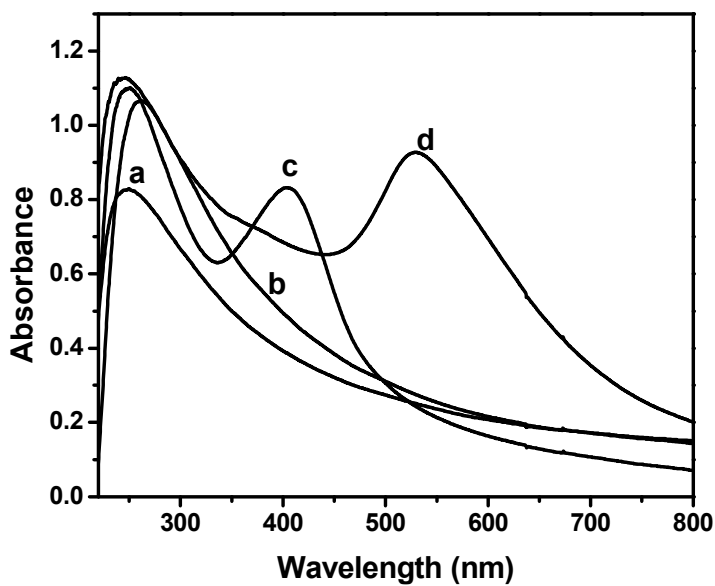


Fig. 5 UV-Vis spectra of (a) GO, (b) GO-Chit, (c) GO-Chit-AgNPs and (d) GO-Chit-AuNPs.

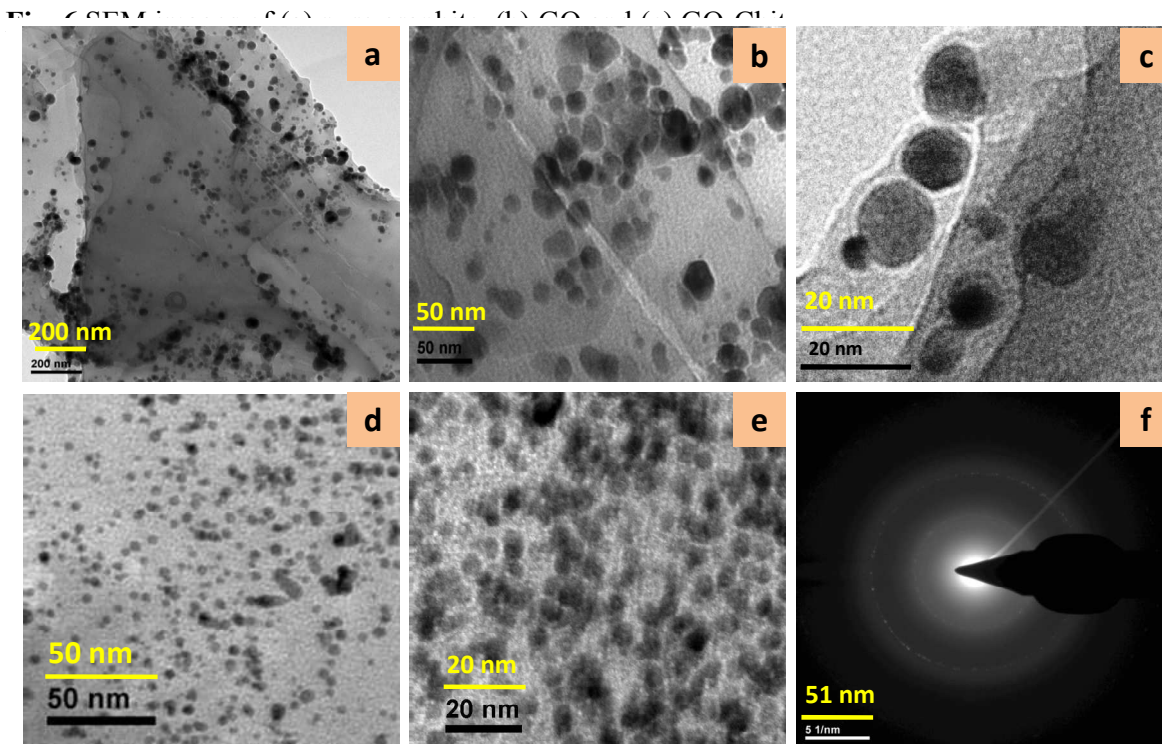
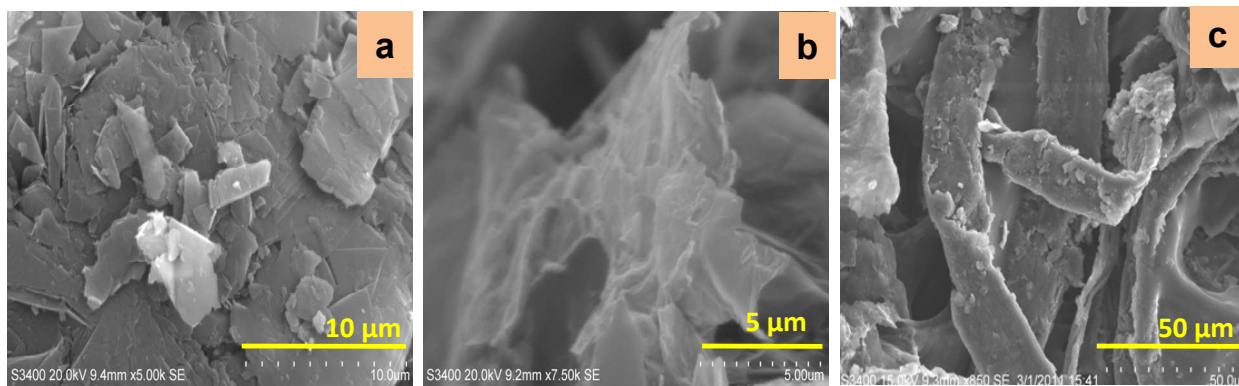


Fig. 7 HR-TEM images of (a, b, c) GO-Chit-AgNPs and (d, e, f) GO-Chit-AuNPs respectively.

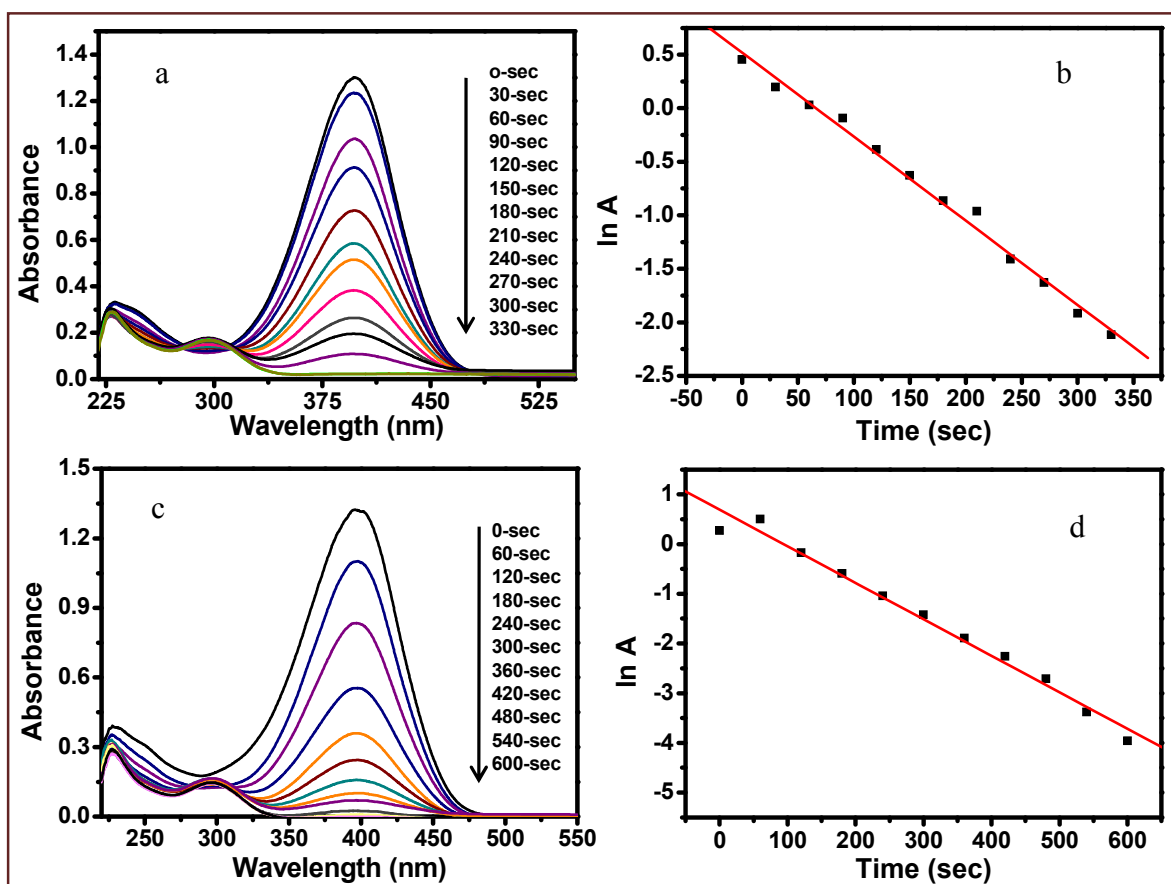


Fig. 8. (a) UV-Vis spectra for the reduction of *p*-nitrophenol measured in different time intervals using (a) GO-Chit-AgNPs, (c) GO-Chit-AuNPs, Fig. 8(b, d) demonstrate ln A vs Time plot for reduction of *p*-nitrophenol Ag/AuNPs decorated GO-Chit respectively.

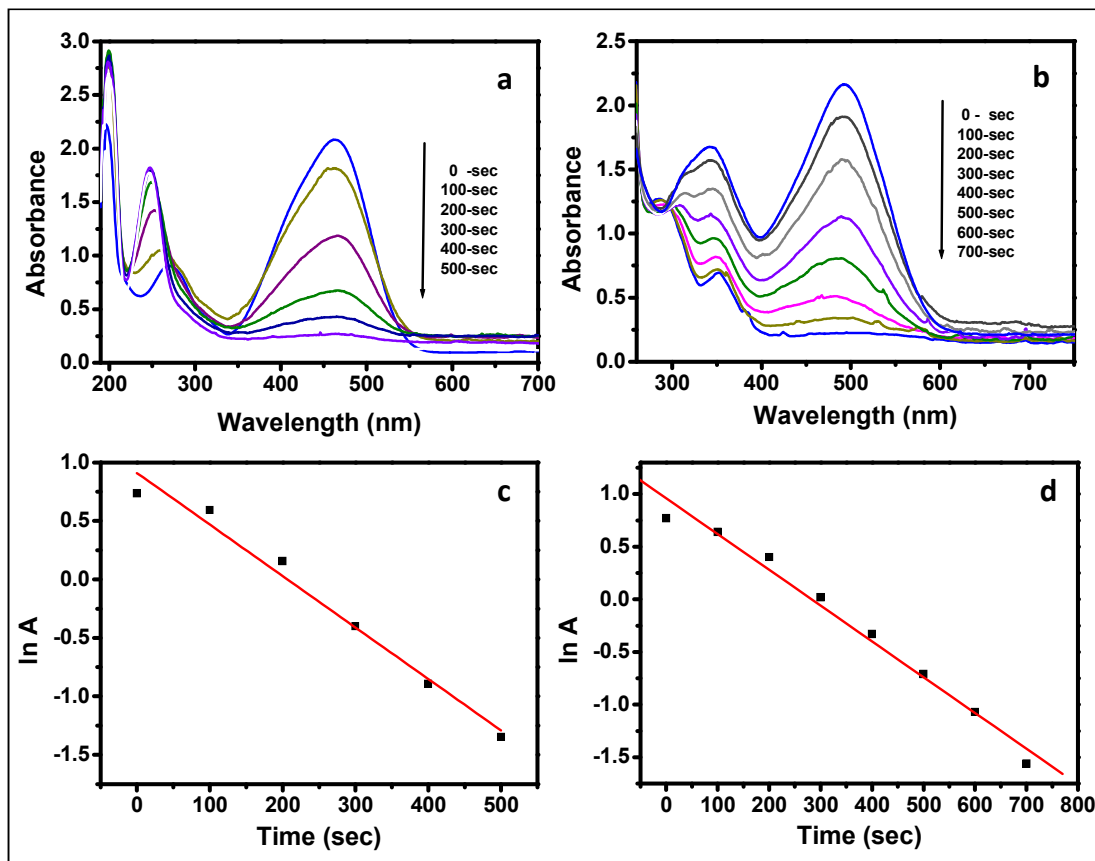
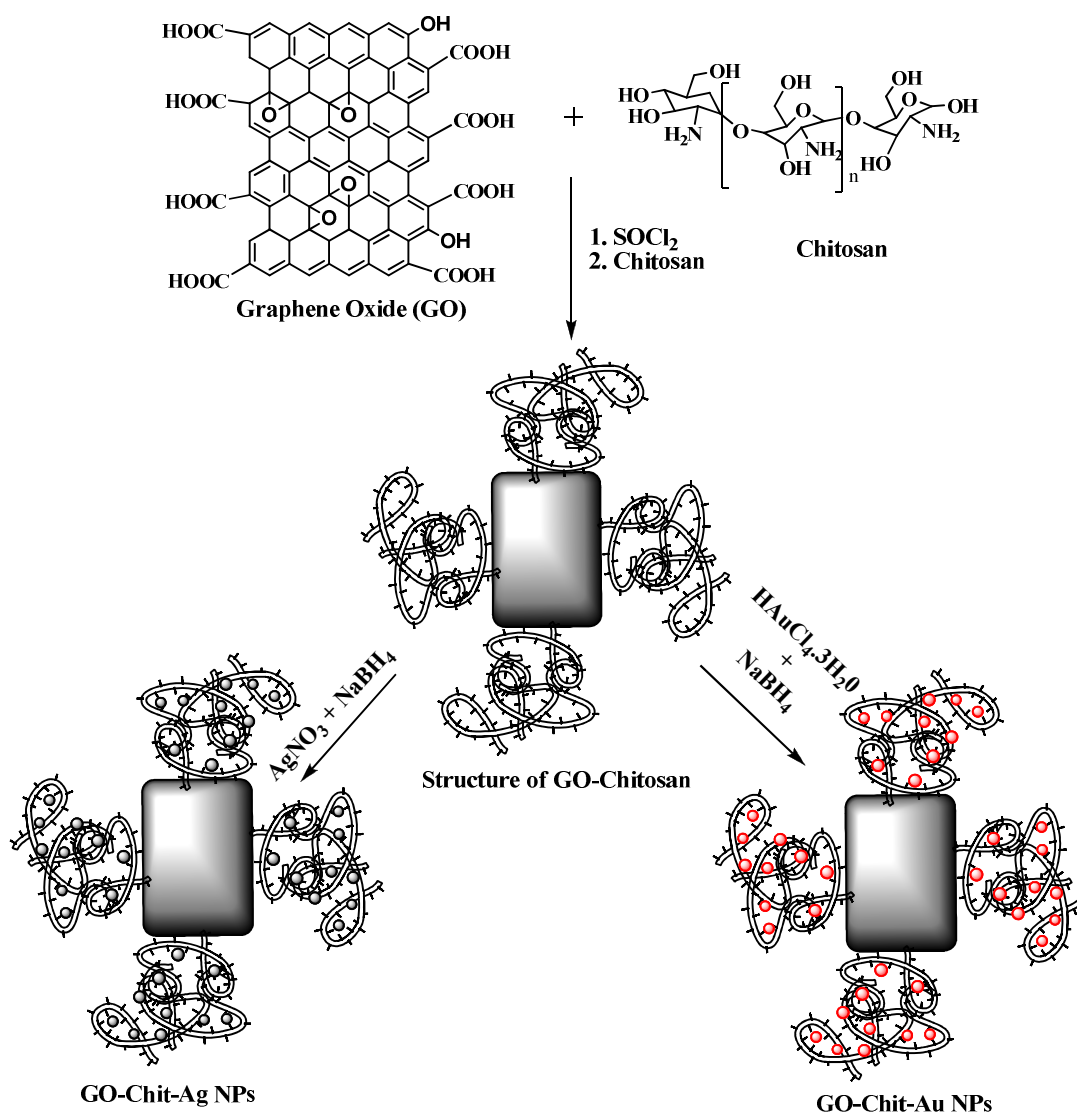
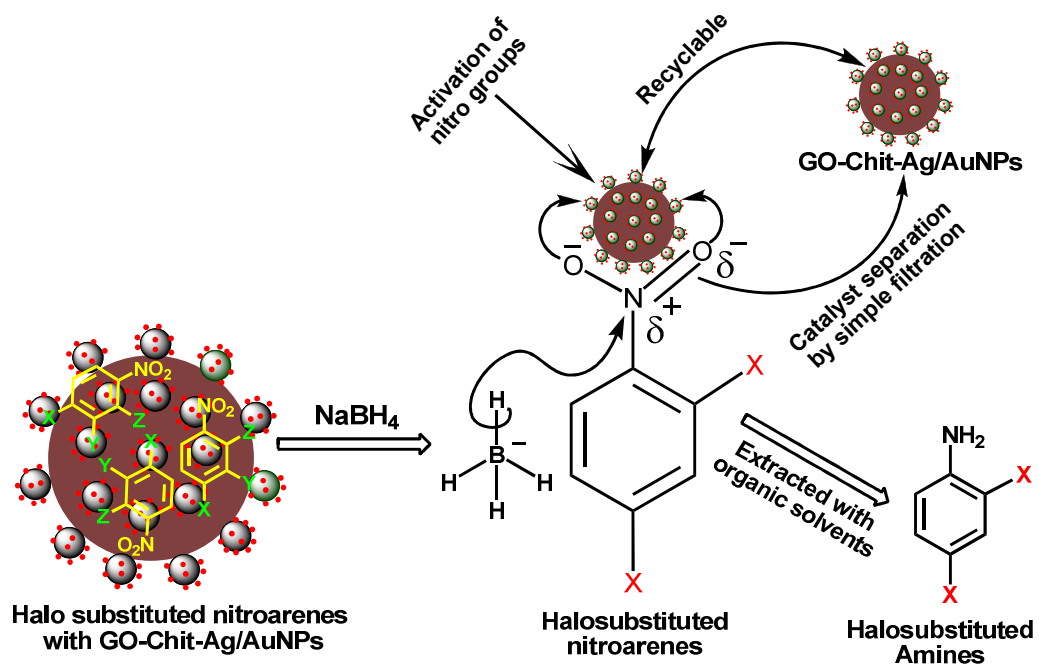


Fig. 9 UV-Vis kinetic spectra for the degradation of (a) methyl orange and (b) congo red by AgNPs-GO-Chit. ln A vs Time plot for the degradation of (c) methyl orange and (d) congo red by AgNPs-GO-Chit.



Scheme 1 Schematic illustration of Ag/AuNPs decorated GO-Chit.



Scheme 2 Plausible mechanism for the reduction of nitroarenes by GO-Chit-Ag/AuNPs

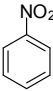
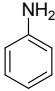
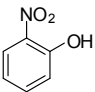
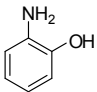
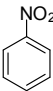
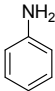
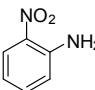
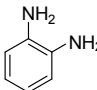
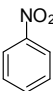
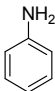
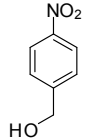
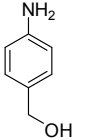
Tables

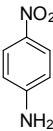
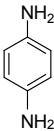
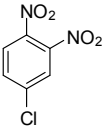
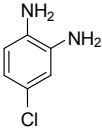
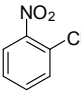
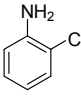
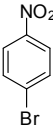
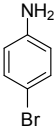
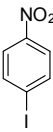
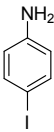
Table 1 Systematic literature survey for the reduction of *p*-nitrophenol and corresponding rate constant at room temperature.

Entry	Sample	Carrier system	Metal	Rate constant (k) for the reduction of <i>p</i> -nitrophenol ^l	Ref.
1	GO-Chit-Ag/AuNPs ^a	Chitosan	Ag	$5.5 \times 10^{-3} \text{ s}^{-1}$	This work
			Au	$3.8 \times 10^{-3} \text{ s}^{-1}$	This work
2	AuNPs/Resin ^b	Ion-exchange resin	Au	$0.16 \times 10^{-3} \text{ s}^{-1}$	19
3	AgNPs/PS-PEGMA ^c	Polymer brush	Ag	$0.33 \times 10^{-3} \text{ s}^{-1}$	20
4	NiNPs/Mesoporous Silica ^d	Silica	Ni	$2.8 \times 10^{-3} \text{ s}^{-1}$	21
5	AuNPs/MgO ^e	MgO	Au	$4.4 \times 10^{-3} \text{ s}^{-1}$	22
6	Pt/Au/Pd NPs/ Silica ^f	Silica	Pt	$0.0014 \times 10^{-3} \text{ s}^{-1}$	23
			Au	$0.71 \times 10^{-3} \text{ s}^{-1}$	
			Pd	$0.715 \times 10^{-3} \text{ s}^{-1}$	
7	AuNPs/Fe ₃ O ₄ ^g	Fe ₃ O ₄	Au	$0.72 \times 10^{-3} \text{ min}^{-1}$	24
8	AuNPs/PEO-b-PAA ^h	PEO-b-PAA	Au	$0.333 \times 10^{-3} \text{ min}^{-1}$	25
9	AuNPs/Breynia rhamnoides ⁱ	Breynia rhamnoides	Au	$4.6 \times 10^{-3} \text{ s}^{-1}$	26

^aReactions were catalyzed by GO grafted chitosan stabilized Ag and Au NPs. ^b Ion exchange resin supported AuNPs. ^c Polystyrene–Polyethylene glycol supported AgNPs. ^dMesoporous Silica supported NiNPs. ^eMagnesium oxide supported AuNPs. ^fPorous silica supported Pt/Au and Pd NPs. ^gIron oxide supported AuNPs. ^hPoly(ethylene oxide)-block-poly(acrylic acid) supported AuNPs. ⁱBreynia rhamnoides in AuNPs. ^lApparent rate constants obtained under optimized conditions. NaBH₄ was used as the reducing agent in all the cases.

Table 2 Catalytic reduction of various nitro aromatics over Ag/AuNPs-GO-Chitosan.

Entry	Substrate	Product	GO-Chit-AgNPs (Time, min)	GO-Chit-AuNPs (Time, min)	Yield ^c (%)
1			40	100	100
2			45	110	100
3			45	110	100
4			45	110	100
5			40	100	100
6			40	100	100

7			45	110	100
8			80	200	66
9			45	120	100
10			45	120	100
11			45	120	100

^aReaction conditions: 50 mg of catalyst, 1 mmol of substrate, 10 mmol of NaBH₄, 50 mL of water, stirring at room temperature.

^bReused catalyst after separation from the reaction mixture.

^cConversion yield was monitored through GC.

Table 3 Systematic literature survey for the degradation of methyl orange and congo red azo dyes and corresponding rate constant at room temperature.

Entry	Samples	Carrier system	Metals	Rate constants (k) for the degradation of		Ref.
				Methyl orange	Congo red ^k	
1	Ag/GO-Chit ^a	Chitosan/GO	Ag	$4.41 \times 10^{-3} \text{ s}^{-1}$	$3.4 \times 10^{-3} \text{ s}^{-1}$	This work
	Au/GO-Chit ^b	Chitosan/GO	Au	$3.01 \times 10^{-3} \text{ s}^{-1}$	$2.14 \times 10^{-3} \text{ s}^{-1}$	This work
2	Ag/Au/Pt/ Tannic acid ^c	Tannic acid	Ag	$583 \times 10^{-3} \text{ min}^{-1}$	-	61
			Au	$4.9 \times 10^{-3} \text{ min}^{-1}$		
			Pt	$2.9 \times 10^{-3} \text{ min}^{-1}$		
3	P25TiO ₂ /GO ^d	P25	Ti	$116 \times 10^{-3} \text{ min}^{-1}$	-	62
4	TiO ₂ /PW ₁₂ ^e	PAH	W	$46.5 \times 10^{-3} \text{ min}^{-1}$	-	63
5	TiO ₂ /CNTs ^f	CNTs	Ti	$37.3 \times 10^{-3} \text{ min}^{-1}$	-	64
6	Alumina/CuO ^g	Alumina	Cu	-	$567 \times 10^{-3} \text{ min}^{-1}$	65
7	Thioacetamide/NiS ^h	Thioacetamide	Ni	-	$72 \times 10^{-3} \text{ min}^{-1}$	66
8	TiO ₂ ⁱ	TiO ₂ (TNA)	Ti	-	$12.5 \times 10^{-3} \text{ min}^{-1}$	67
9	P25TiO ₂ /SiO ₂ ^j	SiO ₂	Ti	-	$0.003 \times 10^{-3} \text{ min}^{-1}$	68

^{a, b}Reactions were catalyzed by GO grafted chitosan polymer stabilized Ag and Au NPs. ^cTannic acid supported Ag/Au/Pt NPs. ^dGraphene oxide supported P25TiO₂NPs. ^eTitanium oxide supported tungsten phosphate nanoparticles. ^fCarbon nanotube supported TiO₂NPs. ^gAlumina supported Copper oxide nanoparticles. ^hNickel sulphate nanoparticles. ⁱTitanium oxide nanotube arrays NPs. ^jP25Titanium oxide NPS supported Silicone oxide nanoparticles. ^kApparent rate constants calculated under optimized reaction conditions. Entries 1, 2 and 6 have utilized NaBH₄ as the reducing agent and entries 3-5 and 7-9 were based on photocatalytic degradation.